Environmental impact of fouling for crude oil flow in preheat pipes according to oil blends

Abdulhussein, Zaid A.; Al-Sharify, Zainab T.; Alzuraiji, Mohammed; Onyeaka, Helen

DOI:
10.1016/j.heliyon.2023.e21999

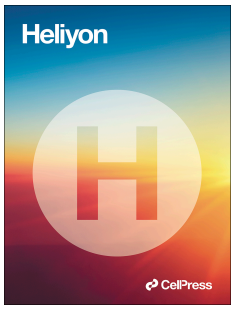

Environmental impact of fouling for crude oil flow in preheat pipes according to oil blends

Zaid A. Abdulhussein, Zainab T. Al-Sharify, Mohammed Alzuraiji, Helen Onyeaka

PII: S2405-8440(23)09207-1

DOI: https://doi.org/10.1016/j.heliyon.2023.e21999

Reference: HLY 21999

To appear in: *HELIYON*

Received Date: 12 May 2023

Revised Date: 26 October 2023

Accepted Date: 1 November 2023

Please cite this article as: , Environmental impact of fouling for crude oil flow in preheat pipes according to oil blends, *HELIYON* (2023), doi: https://doi.org/10.1016/j.heliyon.2023.e21999.

Environmental Impact of Fouling for Crude Oil Flow in Preheat Pipes According to Oil Blends

Zaid A. Abdulhussein [1], Zainab T. Al-Sharify [1,2*], Mohammed Alzuraiji [3], Helen Onyeaka[2*]

[1]Department of Environmental Engineering, College of Engineering, Mustansiriyah University, Baghdad, Iraq
[2]School of Chemical Engineering, University of Birmingham, Edgbaston B15 2TT, Birmingham, United Kingdom
[3]Chief Engineer, Marketing Research SOMO, Iraq

*Corresponding authors: Zainab T. Al-Sharify (z.t.alsharify@uomustansiriyah.edu.iq ; zta011@alumni.bham.ac.uk; z.t.al-sharify.1@bham.ac.uk)
Helen Onyeaka (h.onyeaka@bham.ac.uk)

Abstract

Crude oil fouling is a complex process caused by multiple mechanisms. This study examined fouling's environmental impact on a distillation unit's heating tubes and heat exchangers, proposing optimal pollution levels to reduce emissions and achieve sustainability goals. The study evaluated five crude oil blends in terms of API, sulfur, salt content, and other physical properties. Contaminated water was analyzed through biological and chemical means, while CO2, NOx, and SOx emissions were calculated from actual fuel and power consumption. Solid and sludge sediments were observed throughout all plate heat exchangers, consisting primarily of iron hydroxides and manganese oxides. Rationalizing energy use reduced the burden on the environment and fuel consumption by 7%, with a 2% reduction in energy needed to refine crude oil feeding units when fouling is removed after maintenance. By optimizing pollution levels and reducing energy consumption, the environmental impact of fouling can be mitigated.

Keywords: Fouling; fluid flow; crude oil; environmental pollution; pipeline; carbon emissions

1. Introduction

Understanding crude oil's impact on the environment and daily life has increased, leading to recent environmental engineering advances in oil pollution management and remediation. Global oil pollution has several causes. For decades, petroleum oil contamination has been an issue for the oil sector **[1].** The complicated network of heat exchangers recovers 60–70% of distillation energy, which makes refinery managers prioritise the design and operating efficiency (Figure 1) of a pre-heat train in the crude distillation plant [2]**.** This means that intuitive and analytic optimization of pre-heat trains (PHTs) and careful planning of PHT cleansing are commonplace [3]**.** However, squeeze analysis and other purely heat-integration technologies ignore the gradual decline in performance that contamination causes. Optimal from the standpoint of energy recovery in perfect circumstances but not from the standpoint of operability or, eventually, cost-effectiveness, such a network structure plan may be implemented [4]**.**

Fouling's criticality, its estimated $1 billion price tag in the United States alone during a period of much lower energy has led to its neglect, it appears that no tools can adequately measure it. forecasting the PHT's dynamic fouling behavior. Typically, contamination predictions in refineries are founded on recent patterns. Minimal consideration is given to crude makeup or process conditions, and management choices (e.g., cleaning exchangers, shutting off for maintenance) are often based on basic math and previous experiences [5-7]. Converters in the network are denoted by well-made factors (e.g., geometry). The first step in developing a network model is to connect all streams and exchangers using a common PHT setup and exchanger traits [8**]**.

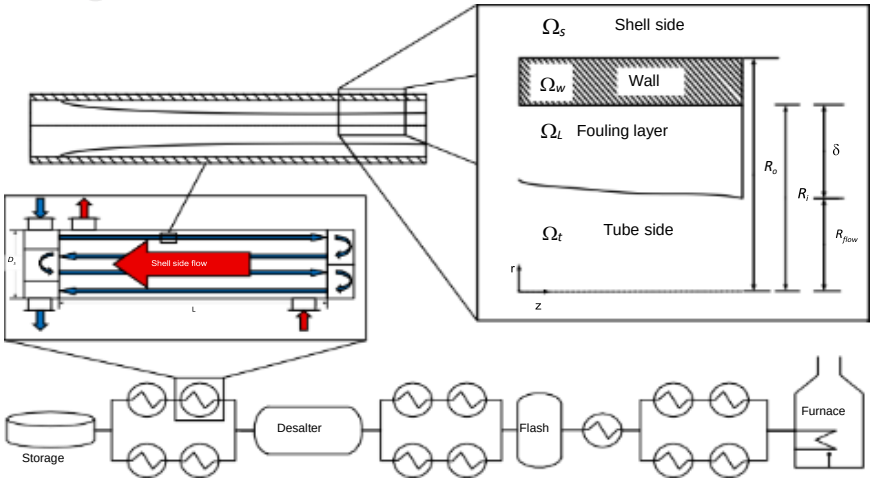

Figure (1) standard pre-heat train equipment model of crude oil fouling [6].

Over the past two decades, increased demand for oil products has rapidly developed the world's petroleum processing capacity [9]. Strong environmental regulations aimed at lowering carbon emissions, which significantly influenced climate change, were connected to an increase in oil use. As a result, paying attention to environmental regulations is essential, which pose significant difficulties for business. Recent work by Abdulhussein et al.,[10] stated that understanding crude oil's environmental impact has led to several modern Environmental Engineering improvements in pollution control and sanitation. Thus, pipeline crude oil fouling issues must be extensively investigated. Heat loss necessitated energy. significantly increased gasoline use and carbon emissions. Pipelines are threatened by rising fluid flow and falling pressure. Iraqi crude oils have minimal asphaltene and impede refinery preheat trains. This article examines fouling of various crude oils and mixes[10]. Essien & John [11] investigate the fouling factor and waxes fouling in oil blends and petroleum exchangers. They explained how fouling is the most significant complication in the petroleum industry and companies. This could prevent process fluids from reaching a suitable temperature. Samimi et al. [12] examined the fouling of heat exchangers in heavy oil systems including asphaltenes and carrier fluids consisting of fuel oil blended with different proportions of aliphatic or aromatic fluids. However, refineries' high runs cause unit fouling. Fouling in preheat trains is likely the main source of refinery energy ineffectiveness, nevertheless, pipeline crude oil flow issues must be investigated [13]. Due to a lack of basic knowledge of the causes, deposition processes, fouling composition, and design effects, this problem has been difficult for decades and requires additional study in numerous countries [14].

The impact of fouling on the soil have not been fully studied over the years however crude oil exploration and other related activities globally have greatly affected the environment with a negative impact on the ecosystem**.** When oil is spilled, its excess leads to saturation of the soil as well as contamination of groundwater. The arrival of saturated hydrocarbon compounds in the soil in the form of crude oil or natural gas affects a "direct" effect on plant cells and leads to a change in soil composition and degree of cohesion and reduces its content. of organic matter**.** Crude oil flowing from crude oil transport pipelines encourages the growth and activity of some microorganisms to convert hydrocarbon compounds into highly toxic compounds that greatly affect other microbial groups spread in the soil. This leads to a reduction in their role in the environmental balance. Soil areas contaminated with crude oil are characterized by a thin black crust of crude oil (tary mat), and contain a

percentage of aromatic compounds in the soil. Studies indicate that the rate of hydrocarbon compounds in some types of soil ranges between (0.02-0.08), while in highly polluted soils this percentage ranges between (0.49-13.22), and this leads to an environmental imbalance [15]**.** Refineries throw large amounts of polluted water due to its entry during filtration processes, which leads to water contamination with pollutants represented in hydrocarbons and oils, and sometimes even a high percentage of oils can be observed [16]. Therefore, fouling impacts the water coming out from refineries as some wastewater treatment systems return wastewater safely to the environment [17]

This work aims to assess the environmental impact of fouling in the heating tubes for heat exchangers of the crude oil distillation unit according to the mixtures and propose the optimal pollution level to reduce fossil fuel emissions, which falls within the sustainable goals. The research dealt with the theoretical study of the acute fouling problems that face the exchangers in the refining unit, which is an urgent problem facing the operators in refineries in general and in the middle refineries (al Daura refinery) in particular and occurs in the heat exchangers, the backbone of the energy supply in the refineries. Furthermore, this study also aims to describe the procedures that eliminates oil pollution at the international and local levels through the study questions that focused on the concept of pollution, the environment, oil, the results of oil pollution, and solutions to avoid it. In addition, The evaluating the fouling in the preheat train of 70 barrel/day distillation unit at Al Daura Refinery, Baghdad, the physical and chemical properties of fouling samples will be examined in order to identify the causes of the issue; Assessing the environmental impact of fouling in terms of air, soil and water; Addressing the energy loss of the distillation unit due to the fouling in the preheat train though determine the additional energy input to the furnace (fuel oil and fuel gas); Estimating the additional CO_2 emission to the atmosphere because of fouling; and Developing recommendations for addressing fouling in preheat trains to improve refinery performance, safety, health, environment, and economy.

2.0 The Environmental Impact of Fouling

Fouling in the heat exchanger is a common issue in the manufacturing industry that hinders both energy recovery and environmental sustainability. A common barrier to effective fouling avoidance is a lack of understanding of the processes at play and pollution's transitory, ever-changing effects on heat exchanger efficiency. More significant pressure loss, increased under-deposit rust, diminished heat transfer, and flow are just some of the practical

severe issues that can arise from fouling in tubes, flow passageways, and other areas of processing equipment [18-20]. Additionally, these editing efforts briefly discuss the environmental effects of heat exchanger pollution, inevitably, the accumulated effect of fouling on a heat exchanger will inevitably vary depending on the intensity of the contamination and the operating circumstances. It is possible, however, to single out a few key features [21-23]

2.1 Economic and Environmental Significance of Fouling

The price of power generation and its impact on the climate determine the fuel the burner needs in addition to what would typically be used. Significant energy losses (pump power) may also result from a rise in pressure decline. Utilizing more gasoline increases CO_2 emissions and their related environmental effect [24]**.** Output losses during fouling-related shutdowns If the furnace restricts the pre-heat train flow, a normal 10% production loss. After manufacturing is resumed, there are extra costs due to out-of-specification output **.** Larger heat exchangers, antifouling equipment, on-line cleansing and treatment devices, larger disposal fees for the (larger) replaced packages**.** The cost of removing fouling layers is normally high and both financial and ecological costs are also linked with improper dumping of cleaning supplies [24].

2.1.1 CO_2 Emissions, Soil and Water Pollution.

The amount of CO_2 released into the atmosphere due to human activity was 2.6 million tons responsible for an estimated 21 years ago, and is anticipated to rise to 4.2 billion tons within seven years [25]**.** Most of these CO_2 pollutants come from burning fossil fuels for transit, heat, and electricity. Fouling affects power, chemical, and hydrocarbon facilities. Heat exchanger contamination releases no quantified CO_2. Some statistics can show heat exchanger fouling's major environmental effect. Before distillation columns, factories heat unrefined oil. The primitive warming train's shell-and-tube heat exchangers do this (CPT). The refinery's energy usage amounts to 6–7% of crude flow, mostly in the CPTs [7, 26]**.** Nearly 750 facilities process 87 million gallons of petroleum oil daily. Refineries use 10–60 CPT heat exchangers. Crude oil contamination accounts for 10% of refineries' CO_2 impact [26]**.** Thus, 186 million gallons of petroleum oil are used annually to counteract pollution, according to a modest calculation. Based on crude oil's 37 MJ/L energy density and heavy oil's 0.28 kg CO_2/kWh (heat) production, pollution emits about 88 million tons of CO_2 per year. 2.5% of human CO_2 emissions come from this. The estimated worldwide economic

effect of heat exchanger pollution is 0.25 percent, making this influence 10 times larger (GDP). Heavy petroleum hydrocarbons that have not been commercially recovered require more complicated refineries [27]. This suggests that CO_2 levels may exceed the positive estimates in this paper. This makes corrosion patterns harder to predict, which increases heat inefficiency and CO_2 release. Since fouling is the biggest element influencing CPT efficiency, there has been a growing emphasis on researching and simulating heat exchanger fouling patterns to better CPT train design and create efficient fouling detection tools [28]. Fouling affects more than oil facilities. Most energy-intensive mass chemical manufacturing methods require heat recovery. Bauxite mines, pulp factories, phosphoric acid facilities, etc. In all situations, extra main fuel must be consumed to mitigate for the detrimental effects of heat exchanger contamination.

3.0 Experimental Work

The methodology of experimental work are presented in Figure 2. Accordingly, the practical work was divided into two sections, and different measurements, including XRF, XRD, EDS, and SEM tests, were applied to analyses the fouling and polluted samples from soil and water samples.

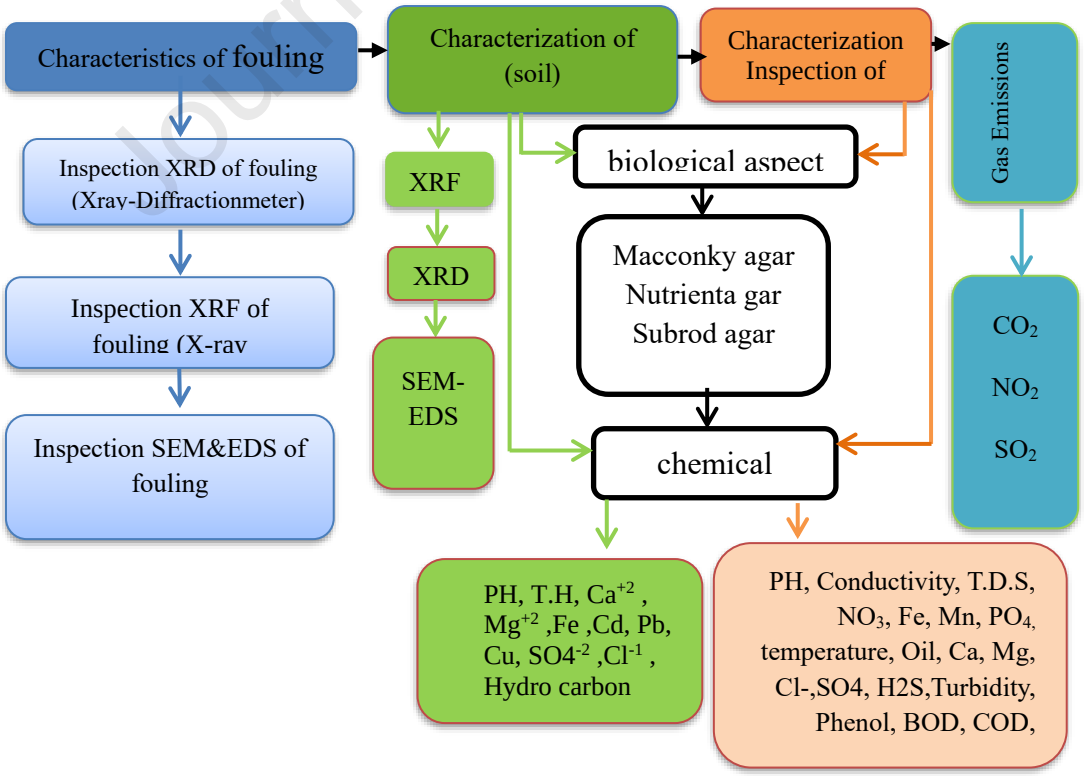

Figure 2 : Diagram of the methodology of experimental work

3.1. Characteristics of Fouling

3.1.1. XRD Fouling Check (X-Ray Diffractometer)

Crystalline forms in materials can be described with the help of X-ray diffraction. In this work, the fouling solid materials were ground into a thin powder as illustrated in **Figure 3(A - F)**, it is then set inside the metal container and polished uniformly until a flat surface emerges**.** The particle was in a small particle size (less than 50 microns), and it must be crystalline. The test was carried out in (college of science, department of Geology, university of Baghdad, Iraq, German laboratory, and ICDD center). **Table (1)** presents the properties of the X-ray diffraction system.

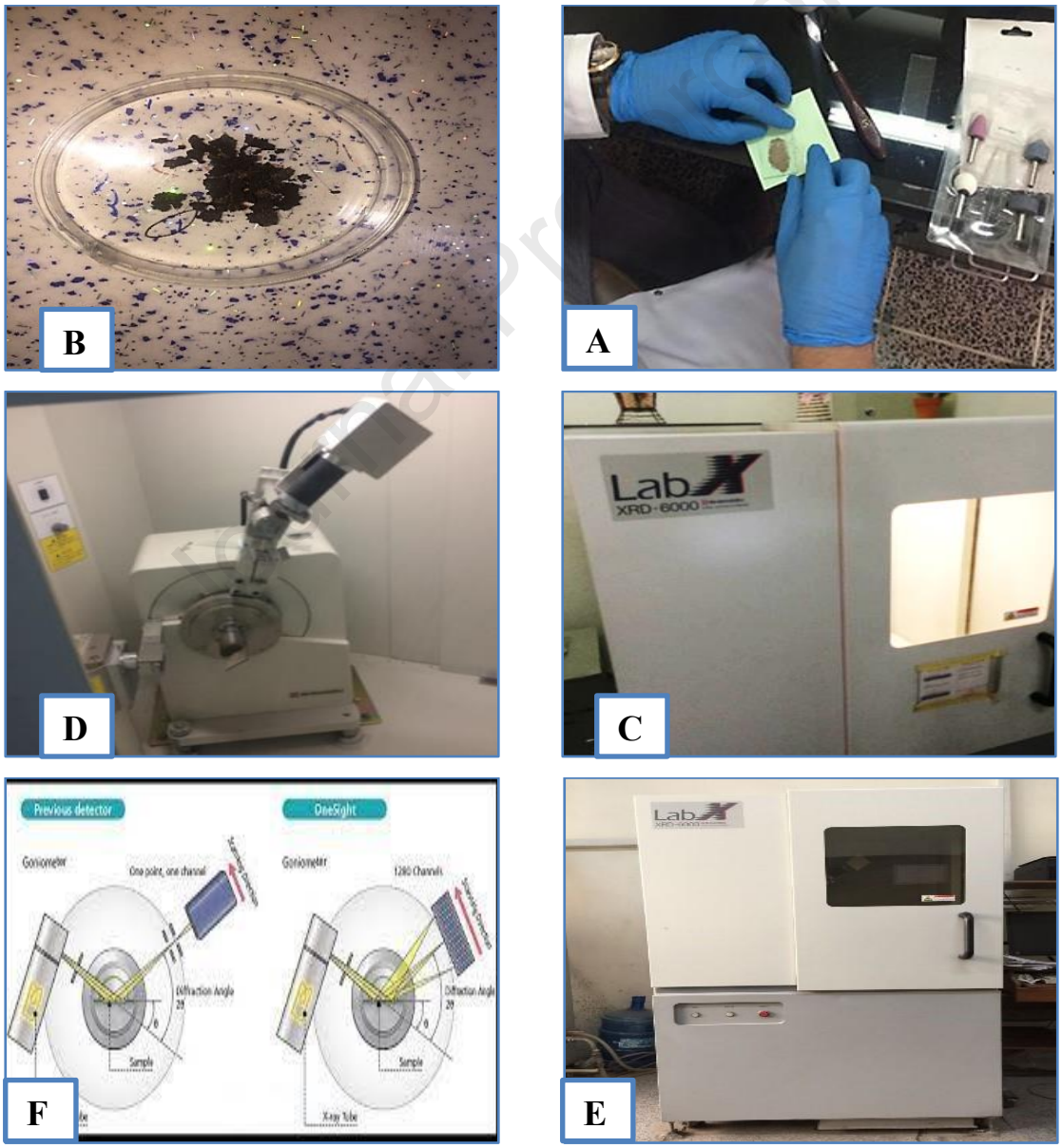

Figure (3) Photographs of the equipment used for the sample preparation for X-ray diffraction research (A) and (B), Shimadzu X-Diffractometer (XRD-6000)

Table (1) X-ray diffraction system.

X-ray diffraction system	
Device type	XRD-6000
the manufacture companies	Himadzu
Origin	Japan
entry voltage	50 HZ/220 V

3.1.2 X-Ray Contamination Examination XRF (X-Ray Fluorescence)

Fouling was examined by XRF technology to excite the process (fluorescence) in the form resulting from electron transitions from one orbit to another in the atomic levels in the sample without damaging the material, and at the same time, Knowing a large number of constituent elements within a sample makes it an excellent method for fingerprinting all types of elements or oxides that make up a fouling sample. Among the advantages of using XRF are fast sample preparation (10–15 minutes), highly accurate results with concentrations ranging from ppm to 100%, and non-destructive or destructive testing of samples and models. As shown in Figure A, the fouling sample was taken using binder (Spectro-approved). The sample is ground using a slurry as shown in **Figure 4 (A-C).** an amount of the fouling sample were taken and placed in the oven to dry it and get rid of moisture (**Figure 1(E&F) supplementary file).** 8 grams of the dried sample were weight and 2 g of it were added to the binder and mixed well **(Figure (g) supplementary file). Moreover,** the sample were pressed in the pressure device to form it into the shape of a hard disk. model (**Figure** 2 & 3 (H, J, K, and L) **supplementary file)**. Finally, the hard disk into the XRF machine to analyze the samples and find the concentrations of the elements. **Figure 4 (M&N&Osupplementary file).**

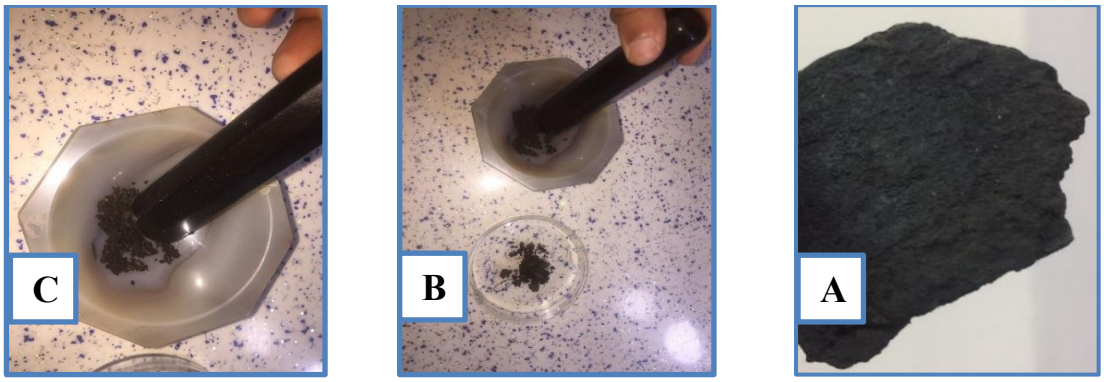

Figure (4) A (sample shell fouling), B&C(mortar).

3.1.3 SEM & EDS Examination of Fouling

Electron microscope analysis was conducted and a SEM picture of the heated sample was acquired at a resolution of 20,000 times. Furthermore, (EDS) was utilized to identify the molecular makeup of the particulate surface. All objects must be desiccated before being analyzed by a scanning electron microscope. Thus, any water resulting from vaporization issues must be removed using the vacuum procedure. This test typically employs a vacuum atmosphere and electrons to create SEM pictures, as Figure (5) in supplementary file depicts**.** Al Khoura Labs in Baghdad, Iraq, was responsible for the testing.

3.2 Evaluation of the Environmental Impact of Fouling

The environmental effects of heat exchanger fouling are studied and it depends on impurities and operation conditions. Physical and chemical characteristics may be used to identify carbon dioxide emissions. In addition, the large amounts of this pollution have the potential to permanently alter the ecosystem and impair human health via increasing fuel use. Inside the furnaces the energy resources used in the Dora refinery (fuel oil, fuel gas, and electricity) were also investigated, depending on the monthly reports provided by the relevant departments, to calculate the total energy consumed in the production process in megajoules.

3.2.1 Gas Emissions

Air pollutants were measured in the Central Refineries Company / Daura Refinery during August 2022, and data were collected and analyzed by mobile environmental laboratory devices according to the periodic monitoring plan. **Figure (6)** in supplementary file shows the devices used to calculate gaseous emissions.

Gaseous emissions are calculated as follows:

Emission weight (Kg) = (M.Wc Ws)M.Ws……(3.10)

Where:

Emission weight (Kg) =Total components weight emitted to air caused by the excess full.

M.Wc: molecular weight of a component (gm/mol).

Ws: substance weight (kg) Ratio of substance* Total fuel mass.

M.Ws: molecular weight of a substance (gm/mol).

Total fuel mass (kg) = V (m^3) fuel (kg/m^3…… (3.11)

Where:

V: Total volume fuel lost m^3.

p fuel: fuel density (kg/m^3).

Specific gravity= *p* fuel (kg/m^3)/p water (kg/m^3) …… (3.12)

Where:

fuel: fuel density (kg/m^3).

water: density of water @ 4C= 1000 kg/m^3

3.2.2 Characterization of the Microstructure of (soil)

In this study, the investigation of the presence of metals responsible for maximum contamination was carried out by microscopic characterization. Also, we visited the Middle Refineries (Al Daura Refinery, Baghdad, Iraq) to examine the polluted area inside and get a good idea of the size and type of pollution as well as the size of the problem and bring samples for examination. Four samples were determined from different areas within the refinery, as follows:

1. Form No. (1):The model is taken from the heat exchanger wash site.
2. Form No. (2):The sample was taken from the soil surrounding the construction site of the refining unit (E10-Czech).
3. Form No. (3): The sample was taken from the soil surrounding the crude oil depot.
4. Form No. (4):The sample was taken from the soil randomly.

The laboratory side included two parts: the biological aspect and the chemical aspect. The samples were cultured for the bacteriological part using the following media Macconky agar, nutrient agar and Subrod agar. An incubator to help provide suitable incubation conditions for microorganisms were used, in addition to the sterilization device (Autoclave)

uses water vapor pressure for sterilization. Moreover, to examine microorganisms, oven for sterilization of glassware, Sensitive balance and the BOD (Biological Oxygen Demand) device. When the samples were brought to the laboratory, an amount of 1 gram of soil was placed in 30 ml of cooled, boiled water, and then work was carried out by planting them in special agricultural media under anaerobic and anaerobic conditions at temperatures of 42 C. In addition, Table 2 presents the comparison of API values for Iraqi crude oils

Table (2) Comparison of API values for Iraqi crude oils

Crude Oil	API
strategic line	27.43
Kirkuk	28.67
Qayyarah	15.52
east of Baghdad	28.29
Basra oil	41.94
Ain Zala	28.49

The chemical composition of the contaminated natural soil (fouling) was examined using X-Ray Spectrophotometry. The chemical structure of the elements and their own compounds was also measured using an X-ray analyzer (SPECTRO XEPOS, Germany).

The samples were analyzed using X-Ray Diffraction to demonstrate the shift in solid form and mineral behavior of copper and iron elements in the earth. The solid materials were ground into a small powder to pass through a US Standard #200 (75 µm) filter. As illustrated in **Figure 5A**, it is then put inside the metal container and polished uniformly until a flat surface is achieved **(Figure 5B).** Consequently, the XRD measurement can effectively evaluate the soil's material composition.

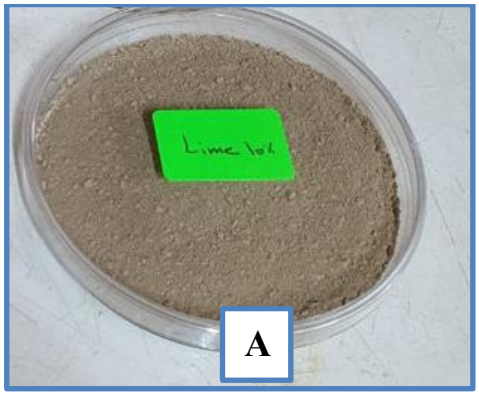

Figure (5) (A) Sample preparation for XRD-diffraction study, (B) Shimadzu X-Diffractometer (XRD-6000).

An electron microscopy examination of soil pollution with components and their oxides has been conducted, and the findings of the XRD method meet some challenges and complications due to the delayed interaction of chemical sections with clay particles in the creation of compounds. A 20,000-magnification SEM picture of the conjunctiva sample is presented below. Further, EDS was utilized to identify the surface's molecular makeup as shown in **Figure 8** in supplementary file; the SEM (scanning electron microscope) is also used to make photos. In Baghdad, Iraq, the Al Khoura Labs conducted tests.

A sample of water contaminated with fouling was taken from the site of washing the heat exchanger **(Figure 6 A & B**), for the characterization Inspection of water and a sample of uncontaminated water was taken before washing the exchanger. Experimental work were conduted to determine the pollutants thrown into the sewage pipes and then into the river, as well as to know the amount of contaminants thrown into the soil and its effect on its mineral behavior. Therefore, For accurate tests, multiple samples of water were taken (before and after washing the heat exchanger) to know the changes that occurred in the water during the treatment process and at separate intervals to determine the quality of this water.

Figure (6) and **(9)** in supplementary file presents the experimental work illustrating the collected sample placed in sterile glass bottles tightly closed with distilled, boiled, and cooled water.

Figure (6) Contaminated water sample from the heat exchanger washing site.

4.0 Result and Discussion

An investigation into the fouling that accumulated in the heat exchanger due to sediment, salts, and high temperatures during the maintenance period's inspection results were disclosed. At the Middle Refineries (Refinery, al Daura), fouling develops due to the heating and cooling of crude oil inside the heat exchanger (E10).

4.1 Characteristics of Fouling

Studying the physicochemical characteristics of crude oil samples entering the (middle) Refineries Company was used to identify the oil from Al-Dura refinery. On December 24, 2022, a sample was obtained from the refinery. The Basra crude oil distillates' weight-to-volume ratios, density, specific weight, API, and sulphur content have all been studied. The findings are presented in tables and graphics.

This work found that Basra oil is a light oil with an API value of 41.9. Sulfur percentages for crude oil in strategic line 3.772 wt %, Kirkuk 2.575 wt %, Qayyarah 6.779 wt %, east of Baghdad 3.12 wt % and Basra 3.055 wt %. The results of the physical standards for the classification of crude oil Basra, the strategic line & eastern Baghdad, the modeling date 26/4/2022. API Gravity @15.6 0c (ASTM-D1298&ASTM-D5002 =28.1), SP. Gravity @15.6 °C /15.6 °C (ASTM -IP, ASTM -D5002 =0.8866), Density @ 15 °C = 0.8861, Sulfur wt. % (ASTM-4294 = 3.50) Kin. Of Viscosity Cs.t (ASTM- D445 = 31.85±0.22 @ 5 °C , 21.9±0. 14 @ 15 °C , 15.48±0.02@ 25 °C , 13.5±0.02@ 35 °C, 11.4±0.02@ 45 °C), Pour Point °C (ASTM – D97 = Bwlow-30), R.V.P Kg /cm^2 @ 37.8 °C (ASTM- D323 = 0.46), Water & Sediment Vol.% (IP-75 =0.25), Wt.% of Salt Content (IP-77 = 0.0196), RCR Wt.% (ASTM -D524& ASTM-D 453 = 6.3), Asphaltenes Content Wt.% (IP 143 = 2.19), Vanadium PPM (ASTM-D6728 = 57.2), Nickel PPM (ASTM D6728 = 16.33), KUOP Characterization Factor (UOP Method 375 = 11.9), Water Vol.% (IP-74 & ASTM- D 4007 = 0.15), Distillation (IP -24), Ash content wt.% (ASTM- D 482 = 0.0080).

It was also found that there is a variation in the concentrations of vanadium and nickel of crude oils entering Iraqi refineries from strategic line, Kirkuk, Qayyarah, east of Baghdad, Basra and Ain Zala. The concentrations of vanadium were (70.74, 22.1, 77.4, 82.6, 57.2,74.4) for each refinary respectively. And the nickel concentrations were found to be (17.96, 14.98, 45.24, 15.58, 16.33, 23.73) for each refinary respectively.

Oils entering the Iraqi refineries from the northern, southern, and central regions, as the Kirkuk refinery were examined. Which contains the lowest concentration of the elements nickel and vanadium less than the rest of the crude oils, and the concentration of vanadium

and nickel in crude oil is more than 2 ppm, it may lead to severe corrosion of turbine blades. A comparison of crude oils entering Iraqi refineries in terms of mineral content (nickel and vanadium), density, API, and sulphur content in the oil

To apply the outcomes of the research study of corrosion products, assessments of an instance of corrosion products deposited on the tube's inside surfacewere made using spectrophotometers. The results of the corrosion products on the the tube's inside surface using spectrophotometers and the analysis show that Na equal to 5150 ppm and the ratio is 0.5; Cl equal to 62000 ppm and the ratio is 6.2; Cr equal to Nil and the ratio is Nil; V equal to 7450 ppm and the ratio is 0.8 %; S^{-2} equal to 3200 ppm and the ratio is 0.3 %; Ni equal to 241.25 ppm and the ratio is 0.02 %; Fe equal to 326614 ppm and the ratio is 32.7 %; Silica and insoluble materials equal to 139000 ppm and the ratio is 13.9 %. In addition, the Asphaltene content for (fouling Sludge) is 3.6609 wt.%.

4.1.1 XRF

Table (3) presentes the XRF results (for the samples taken from the preheat exchanger refining unit-E10- Dora Refinery) indicated that Sodium(0.016 %), Magnesium (0.350 %), aluminum (0.037 %), silicon (0.159 %), phosphorous (0.011%), sulfur (max.2.321%), chlorine (0.119%), potassium (0.013%), Calcium (max.8.069%), manganese (0.013%), iron(max.1.449 %), copper (0.350 %), and zinc (0.102%), strontium (max.0.664%). This result is in disagreement with research [30, 31]

Table (4). shows the chemical analysis, and proportion oxides of the elements such as Na_2O, MgO, Al_2O_3, SiO_2, SO_3, Cl, K_2O, CaO, V_2O_5, MnO, Fe_2O_3, CuO, ZnO, SrO,in different quantities. The heat transfer resistance reduces heat exchanger efficiency as a result of fouling. Hydrochemistry was utilised to investigate the exchange of heat input and output fluids utilising a number of samples. It was discovered that all of the heat exchange plates had crimson stains and easily removed black encrustation. This finding is consistent with [30], as both fouling groups were mostly chemically linked and had somewhat crystalline iron hydroxides and black encrustation that effectively decreased manganese oxide.

Table (3) show that Zn and Mg is found in small quantites, simillarly Al, Si, Ca, Na, Sr, K, Cu, while Iron was bounded organically and as amorphous/ slightly crystalline iron hydroxides.

Table (3) XRF for Elemental Concentrations (Shell Fouling solid).

Name	Z(Atomic number)	Value
Na	11	0.016 % =11.6
Mg	12	0.350 % = 35
Al	13	0.037 % = 3.7
Si	14	0.159 % = 15.9
P	15	0.011 % = 1.1
S	16	2.321 % = 232.1
Cl	17	0.119 % = 11.9
K	19	0.013 % = 1.3
Ca	20	8.069 % = 806.9
Mn	25	0.013 % = 1.3
Fe	26	1.449 % = 144.9
Cu	29	34.349 PPm
Zn	30	0.102 % = 102.2
Sr	38	0.664 % = 66.4
Note/ the percentage can be converted to (ppm) by multiplying the extracted value by (10,000)		

Table (4) XRF for Elemental Concentrations (Shell Fouling solid).

Name	Z(Atomic number)	Value
Na_2O	11	0.694
MgO	12	6.334
Al_2O_3	13	0.609

SiO_2	14	2.341
SO_3	16	22.849
Cl	17	0.476
K_2O	19	0.082
CaO	20	53.681
V_2O_5	23	0.045
MnO	25	0.075
Fe_2O_3	26	10.384
CuO	29	0.026
ZnO	30	0.541
SrO	38	1.758
Note/ the percentage can be converted to (ppm) by multiplying the extracted value by (10,000)		

4.1.2 X-Ray Diffraction (XRD)

X-rays analysed the chemical composition of the crystalline phase mixture shown in **Table (5),** which appeared here in the form of magnesiocalcite **(**$Mg_{0.06}Ca_{0.94}$**),** carbon trioxide (CO_3), and copper silicon sulphide (Cu_2SiS_3**)**, the results is in agreement with Helalizadeh et al. [32]. Then, the composition of these sediments was determined using a coherent laser scanning method, the thickness of the sediment along and around the probe was measured, allowing for a correlation between the probe's temperature data and oil and sediment from various process circumstances. Chew et al. [33] state that in order to differentiate between the most prevalent crude oil contamination processes, a simple approach similar to that suggested by Brons et al. [34] is adequate to predict only a few components.

Possibly better understanding the fundamental processes involved in the creation of expelled deposits could be gained through analysis of particles produced in laboratory experiments. However, due to the intricacy of crude oil production, the frequent change of feedstocks, and the considerably lengthy stages of contamination build-up, it is difficult to recreate the circumstances leading to accumulation in laboratory testing (months or years).

Getting accurate findings calls for a methodical gathering of contamination samples from the refinery's heat exchangers, with consideration given to fluid characteristics and working circumstances. Liquid hydrocarbons can leave behind various contaminants in their wake, including inorganic and organic molecules. Since typical analytical methods can not be used due to their poor solubility, proper sample preparation procedures are necessary before chemical analysis occurs [35].

Table (5) The mineral phases of the analytical technique using X-ray diffraction using an X ray.

Peak ID Extended Report (11 Peaks, Max P/N = 9.6)									
[1.mdi] ADX-2700 SSC 40kV/30mA Slit:1deg&1deg&0.2mm Monochromator: ON Ts-Td									
PEAK: 15-pts/Parabolic Filter, Threshold=3.0, Cutoff=0.1%, BG=3/1.0, Peak-Top=Summit									
36.205	2.479	46	12	(Mg0.06Ca0.94)(CO3)	2.4815	13.6	(1 1 0)	36.168	-0.037
39.747	2.2659	86	22.5	(Mg0.06Ca0.94)(CO3)	2.2722	17.6	(1 1 3)	39.633	-0.115
43.398	2.0834	61	16	(Mg0.06Ca0.94)(CO3)	2.0832	14.5	(2 0 2)	43.402	0.004
47.891	1.8979	65	17	(Mg0.06Ca0.94)(CO3)	1.901	18.1	(0 1 8)	47.806	-0.084
48.987	1.8579	60	15.7	Cu_2SiS_3	1.8635	13.4	(2 0 2)	48.83	-0.156
58.011	1.5886	23	6	Cu_2SiS_3	1.5892	9.3	(3 3 1)	57.986	-0.025
61.417	1.5084	19	5	(Mg0.06Ca0.94)(CO3)	1.5091	2.1	(2 0 8)	61.385	-0.032
61.479	1.507	18	4.7	Cu_2SiS_3	1.507	0.6	(-2 6 2)	61.479	0

2-Theta	d(?)	(h k l)	BG	Height	I%	Area	I%	FWHM	XS(nm)
23.244	3.8236	(0 1 2)	5	49	12.8	250	7	0.217	37
29.602	3.0152	(2 0 0)	11	382	100	3549	100	0.395	20
32.902	2.7199	(-2 2 1)	7	19	5	52	1.5	0.116	73
36.205	2.479	(1 1 0)	11	46	12	326	9.2	0.301	27
39.747	2.2659	(1 1 3)	10	86	22.5	630	17.8	0.311	27
43.398	2.0834	(2 0 2)	5	61	16	524	14.8	0.365	23
47.891	1.8979	(0 1 8)	12	65	17	751	21.2	0.491	17
48.987	1.8579	(2 0 2)	7	60	15.7	1128	31.8	0.799	10
58.011	1.5886	(3 3 1)	7	23	6	147	4.1	0.272	33
61.417	1.5084	(2 0 8)	6	19	5	193	5.4	0.432	21
61.479	1.507	(-2 6 2)	6	18	4.7	215	6.1	0.508	18

4.1.3 SEM-EDX TEST for the fouling heat exchangers

The results of SEM-EDX tests are shown in **Table (6)**. After analysis of the solid samples taken from the heat exchanger plates, **Figure (10)** highlights the main structures evident in the images and the physical boundaries between the two metallic phases. A dark black sediment is shown by the branching structure in the top section of the image. Up to 56.9% carbon, 3.1% iron, 12.5% oxygen, 9.5% calcium, 2.3% aluminum, 8.9% silicon, 1.4% magnesium, 4.9% sulphate, and 0.5% potassium are present in this fraction, which has a forked (crystalline) surface. The next layer corresponds to the red sediment are shown in the Image Zoom Scale (50μm) as shown in **Figure (7&9)**. Thus, these results support the sequential extraction of orange-red paints that are applied to dark brown paint rich in manganese and contain more iron, arsenic, and (organic) carbon. After cleaning, the high-pressure water-removable red sediment and black crust at the bottom remained. These two sediments were too thin to sample for separation. Reddish and black deposits had been predominantly crystalline iron and arsenic hydroxides, with a few trace amounts of iron, manganese, and zinc (**Figure 20**). The bulk of arsenic forms were discovered to bond with ion hydroxides, which agrees with the research of Greif [36] & Epstein [37]**.** SEM shows that manganese-rich regions are more crystal-like than iron-rich ones (**Figures** (**7&8**)). Amorphous iron hydroxides often topped manganese-rich encrustation. Exchanger plates may layer magnesium hydroxide crystals.

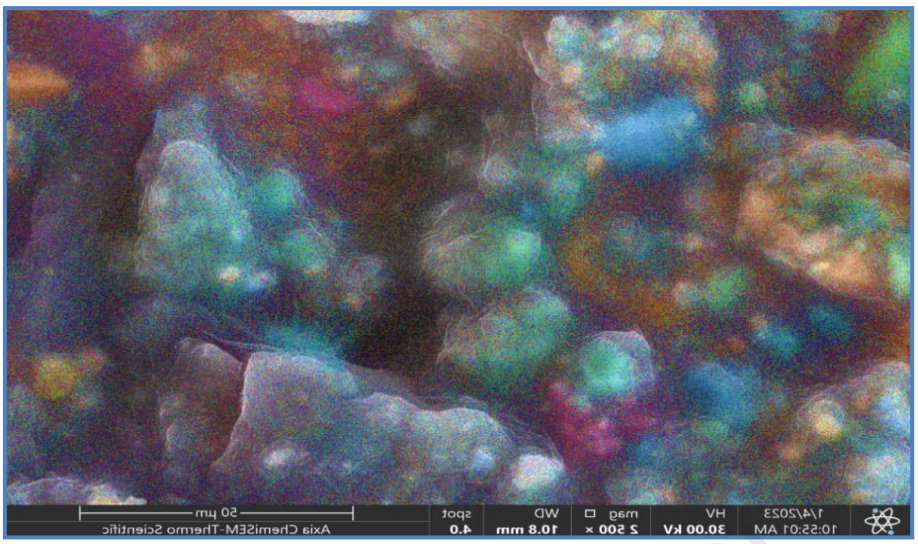

Figure (7) Image Zoom Scale (50µm).

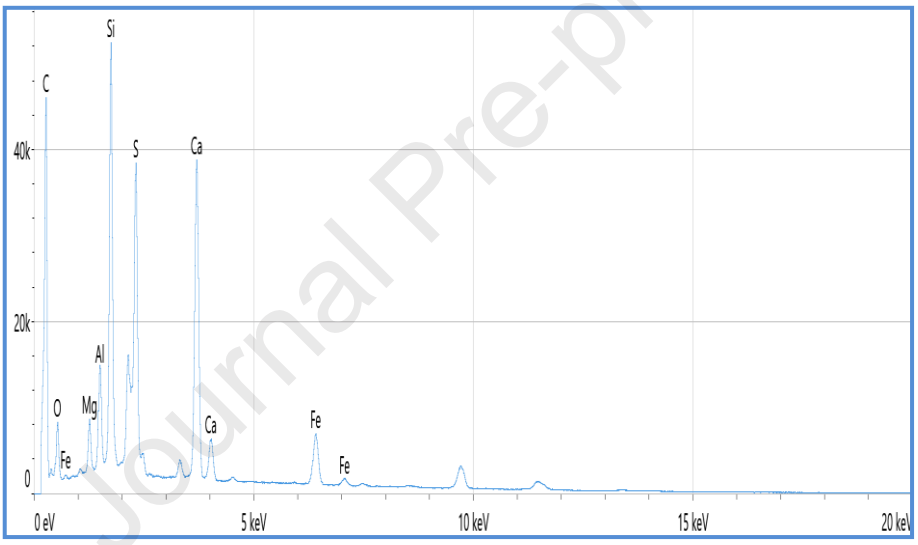

Figure (8) The concentrations of the elements by **SEM-EDS** examination carried out in Al-Khora laboratory (Baghdad - Iraq).

Table(6) EDS images for the untreated contaminated sample(fouling).

Element	Atomic %	Atomic % Error	Weight %	Weight % Error
C	73.7	0.3	56.9	0.3
O	12.1	0.1	12.5	0.1
Mg	0.9	0.0	1.4	0.0
Al	1.3	0.0	2.3	0.0

Si	4.9	0.0	8.9	0.0
S	2.4	0.0	4.9	0.0
K	0.2	0.0	0.5	0.0
Ca	3.7	0.0	9.5	0.0
Fe	0.9	0.0	3.1	0.0

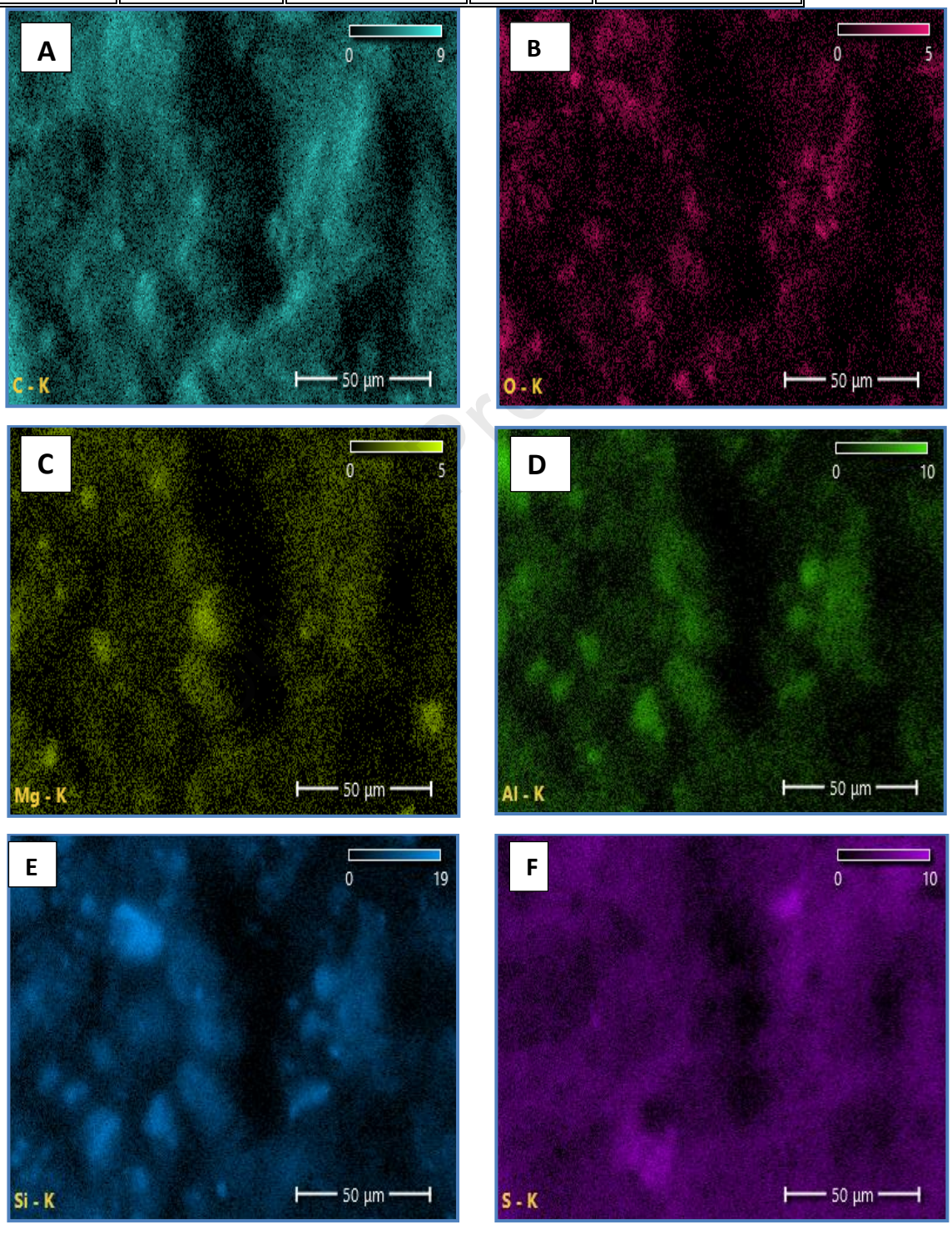

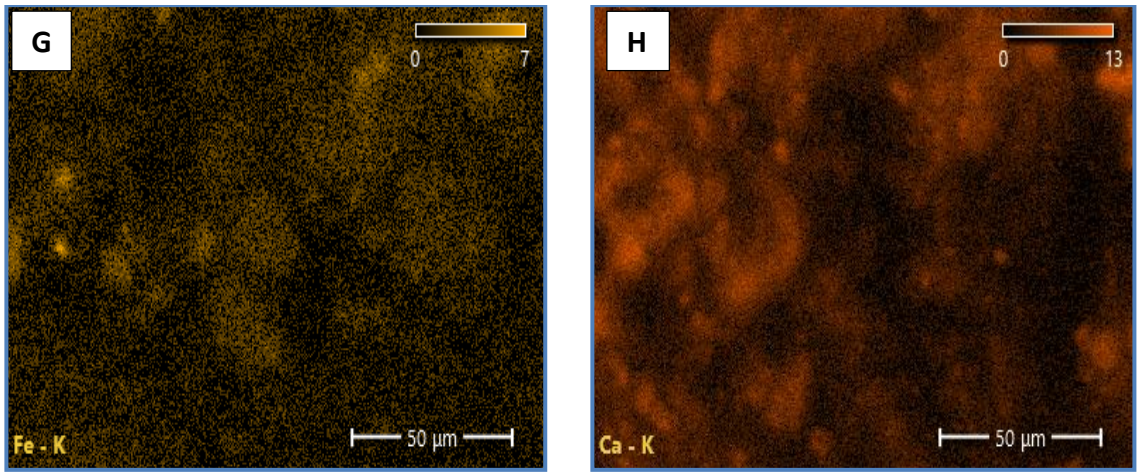

Figure (9) (SEM-EDS) Image shows each element in the fouling; **A)** C element, **B)** O element, **C)** Mg element, **D)** Al element, **E)** Si element, **F)** S element.

The EDS results show that all the samples contain C, O, Mg, Al, Si, S, K, Ca, and Fe. Many elements of Al (**Figure 9 D**) and Si (**Figure 9 E**) agree well with the XRF results and shows well distribution of element C element as seen in **Figure 9A**. The observed phenomenon exhibits a deficiency in the complete combustion of residual carbon., this result is in agreement with the research [30]**.**

4.2 Evaluation of the Environmental Impact of Fouling

4.2.1 CO2 Emissions

Table (8&9) shows the quantities of energy sources consumed at the Dora refinery, the costs involved, and the amount of energy spent per cubic meter of crude oil, Expenditures of energy quantities (fuel oil, fuel gas, naphtha, electricity) with the costs resulting from their consumption for the month of August. The amount of energy needed to refine a cubic meter of refined crude oil was calculated for the month of August and is equal to **165 MJ/m^3**. This was compared with the average standard value of energy required to refine a cubic meter of crude oil, which was calculated at a limit of **2299 MJ/m^3**, also been calculated amount of reductive emissions for month August at the Dora refineryas shown in **Table 9.** We notice a rationalization in the amount of energy spent. by **7%**, which reduces the burden on the environment and the amount of fuel consumed. **Table (7)** shows the actual consumption of total energy per feed unit was calculated using:

1. The actual consumption of the total energy per feeding unit (for the current month) (Mj/m^3) = $\frac{\text{Total energy consumed (Mj)}}{\text{refined crude oil (m3)}}$ …….. (4.4)

2. The cost of energy required to refine each cubic meter of crude oil (M^3/ID) = $\frac{\text{Total cost of energy consumed (ID)}}{\text{amount of crude oil } (m3)}$ …… (4.5)

3. The difference in total energy consumption per feed unit between two months (MJ/m3) is equal to the previous month's total energy consumption per feed unit (MJ/m3). Actual consumption of total energy per feed unit for the current month (MJ/m^3)
4. The difference in the amount of nutrients between two months (m3) is equal to the amount of feedstock (refined crude oil) for the previous month (m3) and the amount of feedstock (refined crude oil) for the current month (m3).
5. Extra energy used per cubic meter of crude oil this month equals the difference in the amount of nutrients (in m3) times the amount of energy used (in MJ/m3) between the two months.
6. This month's additional fuel oil consumption (m3) = this month's additional energy consumption per cubic meter of crude oil (38680 MJ/m3).
7. The increase in the economic value of fuel oil during this month (ID) = the amount of additional oil used during this month (m3) times the price of one cubic meter of fuel oil.

Table (7) Conversion factor.

Conversion factor		
Heat value: fuel oil (m^3)		38680 MJ/m3
Heat value: fuel gas (m^3)		37 MJ/m^3
Electricity (Kw.hr)		10.5MJ/m^3
Naphtha		32239.9 MJ/m^3
Item	**density**	**Heat value**
Gas oil	850 Kg/m^3	108000 Kcal/kg, 384366.6 MJ/m^3
Naphtha	700 Kg/m^3	11000 Kcal/Kg, 32239.9 MJ/m^3

Table (8) Consumed quantities of energy sources and their cost for the month of **August** after cleaning at the Al Daura refinery.

Energy Sort	Unit	Quantity	Quantity of Energy in MJ	MJ	Cost%
Fuel Oil	m^3	1231	47615080	90%	29%
Fuel gas	/1000m^3	1265	46805	0.09%	20%
Naphtha	m^3	0	0	0%	0%
consumed electricity	Kw.hr	502367	5124143	10%	51%
Crude Oil	m^3	320018	/	/	/
Energy consumed per unit feed of crude oil	MJ/ m^3	165	/	/	/
Cost of energy required to refine each cubic meter of crude oil	ID/ m^3	387	/	/	/

Table (9) Amount of reductive emissions for month **August** at the Al Daura refinery.

CO_2	Ton	750
NO_2	Kg	1223
SO_2	Ton	23

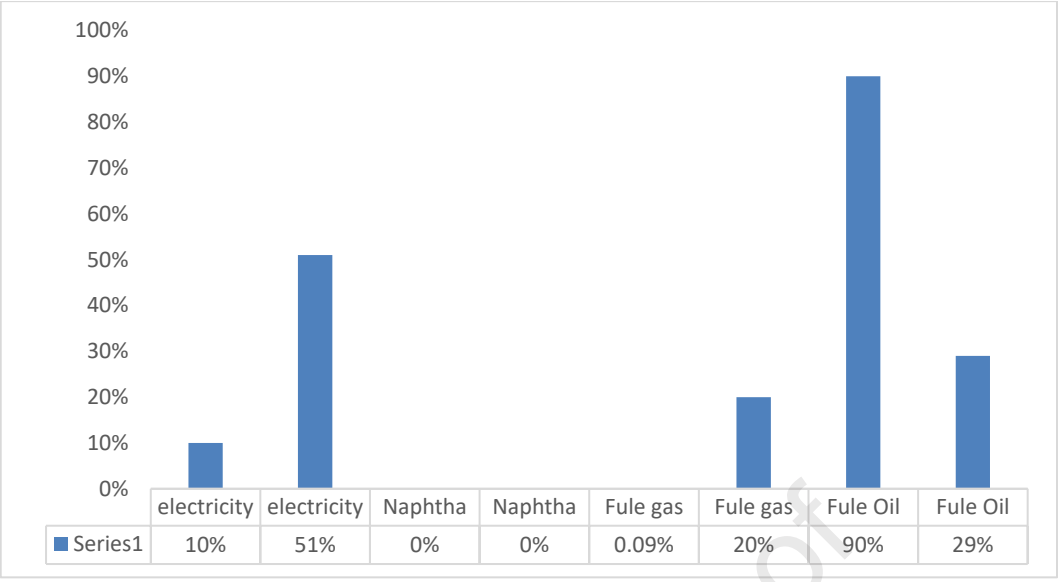

Figure (10) The difference in energy consumed from the standard value (MJ/m^3).

The company's energy consumption rate and value **(2299 MJ/m^3)** were calculated, as the best two years of energy values recorded for the years **(2016-2019)** were adopted and considered a standard value to be compared. **Figure 11** shows the percentage difference between the energy consumed for August and the standard value of energy expenditures for the Al Daura refinery.

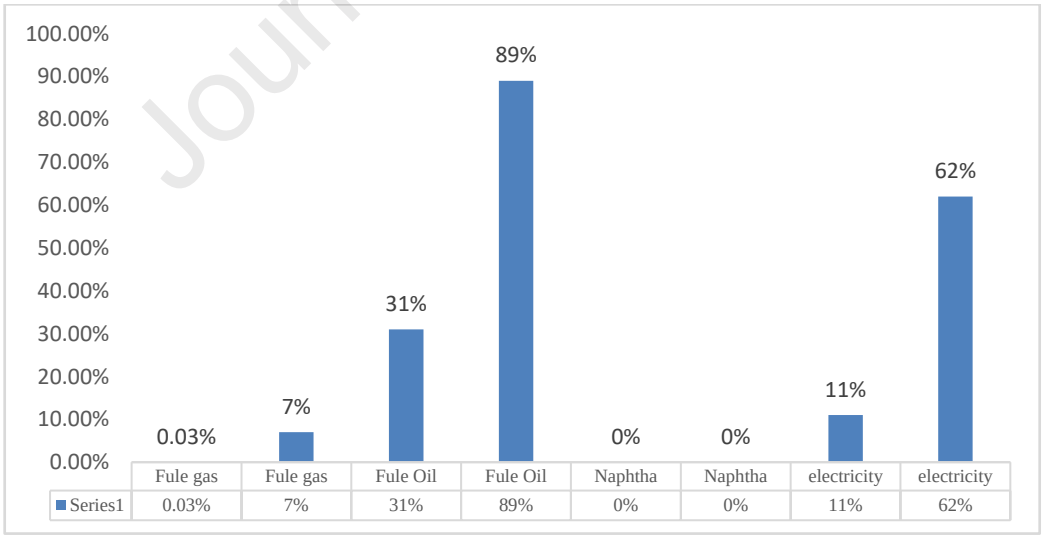

Figure (11) The difference in energy consumed from the standard value (MJ/m^3).

Table (10) The amount of fuel consumed by refining units (1) from 1/1/2022 to 12/31/2022.

M onth	refining unit CR1-70000 (m3)							
	Fule gas	SO_2	NO_2	CO_2	Fule oil	SO_2	NO_2	CO_2
January	962.402	0.0126	0.0094	4.41	1135	0.1	0.01	2.7
Februar y	1214.359	10.06	11.97	5620.3	1182	98.1	8.9	2237.1
March	1217.617	12.2	12.01	5538.6	125	95.8	8.6	3011.5
April	1004.238	4.6	9.89	5089.3	1173	92.2	8.9	3241.9
May	128.800	8.2	1.2	5118	157	3.9	1.2	416.5
June	1231.655	17.6	12.1	5727.02	1216	106.4	9.3	3313.8
July	1236.858	14.1	12.2	6403.6	1226	105.03	9.3	3342.8
August	1265.308	8.3	12.5	6639.8	1231	106.3	9.3	3348.6
Septemb er	1123.255	11.2	11.1	5651.7	1252	111.8	9.5	3411.1
October	1035.483	8.9	14.1	5608.01	1226	109.6	9.3	3340.1
Novemb er	1369.409	7.04	13.5	8238.9	1259	112.2	9.6	3431.8
Decemb er	1118.456	8.3	11.02	6381.7	1147	81.5	7.1	2553.7
Total	12907.840 (m^3)	110.5126 Ton	121.5994 Kg	66021.34 Ton	13329 (m3)	1022.93 Ton	91.01 Kg	31651.6 Ton

Table 11 and **Table 12** shows the quantities of energy sources consumed at the Daura refinery, the costs involved, and the amount of energy spent per cubic meter of crude oil, Expenditures of energy quantities (fuel oil, fuel gas, naphtha, electricity) with the costs resulting from their consumption and the amount of emissions from the furnaces according to the amount of fuel consumed in the first refining unit. for **April**. The amount of energy needed to refine a cubic meter of refined crude oil was calculated for **April** and is equal to **168 MJ/m^3**. This was compared with the average standard value of energy required to refine a cubic meter of crude oil, which was calculated at a limit of **2299 MJ/m^3** and also calculated amount of reductive emissions for August at the Dora refinery's shown in **Table (9)**. We notice a rationalization in the amount of energy spent. by **7.3%**, which reduces the burden on the environment and the amount of fuel consumed.

Table (11). The consumed quantities of energy sources and their cost for the month of **April** before cleaning in the refining unit CR1-70000.

Energy Sort	Unit	Quantity	Quantity of Energy in MJ	MJ	Cost%
Fuel Oil	m^3	1173	45371640	92%	33%
Fuel gas	/1000m^3	1004,238	37157	0.08%	19%
Naphtha	m^3	0	0	0%	0%
consumed electricity	Kw.hr	404574	4126655	8%	48%
Crude Oil	m^3	294966	/	/	/
Energy consumed per unit feed of crude oil	MJ/ m^3	168	/	/	/
Cost of energy required to refine each cubic meter of crude oil	ID/ m^3	355	/	/	/

Table (12) The amount of emissions from the furnaces according to the amount of fuel consumed in the first refining unit for month **April**.

CO_2	Ton	829
NO_2	Kg	1352
SO_2	Ton	25

Table (13) Maximum concentration of air pollutants in Los Angeles, USA

polluter	maximum allowable concentration (ppm)		
	warning	Emergency	Danger
Carbon monoxide	100	200	300
Nitrogen oxides	3	3	10
Sulfur dioxide	3	3	10

Mathematical of the gas emission equation from the furnaces and chimneys at the Al Daura refinery was conducted for August 2022, depending on the fuel consumption rates provided by the operational departments at the Al Daura refinery, and the results were as shown in **Figure 12.**

1. The area with the most pollution outside of the refinery was near the highway next to the refinery. This is because the highway was on the pollution spread line, and the wind was blowing in that direction most of the time, Therefore, the concentration values were high and outside the determinants, as shown in **Figure 12**
2. A random critical point was taken in region No.7, and the results were analysed mathematically. It was found that it was within the permissible limits (**59.667 ppm**) for sulphur oxides, and the allowable limits were 150 ppm. as well as nitrogen oxides were within the permissible limits (**29.407 ppm**) and the permissible limits (**50 ppm**). The analysis was conducted based on the worst weather conditions, where the wind direction was southwest, which occurred **16** times only during the month of August.
3. A critical point was taken near the residential houses near the Al Daura refinery and found that it is within the permissible limits (**8.115ppm**) for sulphur oxides and the permissible limits are 150 ppm, while nitrogen oxides were within the permissible limits at (**1.217 ppm**) and the permissible (**50 ppm** (as the direction of the wind was north-easterly, i.e., **16** times only during the month of August

Constituent	S1	S2	S3	S4	S5	S6	S7	S8	S9	S10
CO2 gr/s	9.078898936	2443.009847	3784.221289	912.8821342	295.5003734	999.2447779	0	303.4968571	10359.04997	147709.8016
SO2 gr/s	0.032499253	11.1834955	48.36475673	4.178887201	9.439151285	31.92214444	0	9.6945825	330.8985324	677.0939051
NO2 gr/s	0.02289614	3.36757766	4.674406923	1.25834782	3.469167139	2.815759625	0	3.563045662	121.6149927	49.94872612

Concentration in PPB				
constituent	District NO.7	houses near the Dora refinery	Highway adjacent to the refinery	Limit/hr.
CO2 (PPB)	3389.775082	3405.435434	15746.98661	(Additional)
SO2 (PPB)	59.66764791	8.115415281	1904.276213	150
NO2 (PPB)	29.40706637	1.217965419	288.4998661	50

position	wind angle	Effective period time (times/month)
A random point in District 7	225 SW	16
houses near the Al Daura refinery	45 NE	2
Highway adjacent to the refinery	315 NW prevalent	most of the month

Date	times	
	45 degree	225 degree
1-Aug	0	0
2-Aug	0	0
3-Aug	2	0
4-Aug	0	0
5-Aug	0	0
6-Aug	0	5
7-Aug	0	0
8-Aug	0	0
9-Aug	0	0
10-Aug	0	0
11-Aug	0	0
12-Aug	0	0
13-Aug	0	4
14-Aug	0	0
15-Aug	0	0
16-Aug	0	0
17-Aug	0	0
18-Aug	0	0
19-Aug	0	0
20-Aug	0	0
21-Aug	0	0
22-Aug	0	0
23-Aug	0	3
24-Aug	0	0
25-Aug	0	0
26-Aug	0	0
27-Aug	0	0
28-Aug	0	0
29-Aug	0	0
30-Aug	0	0
31-Aug	0	4
	2	16

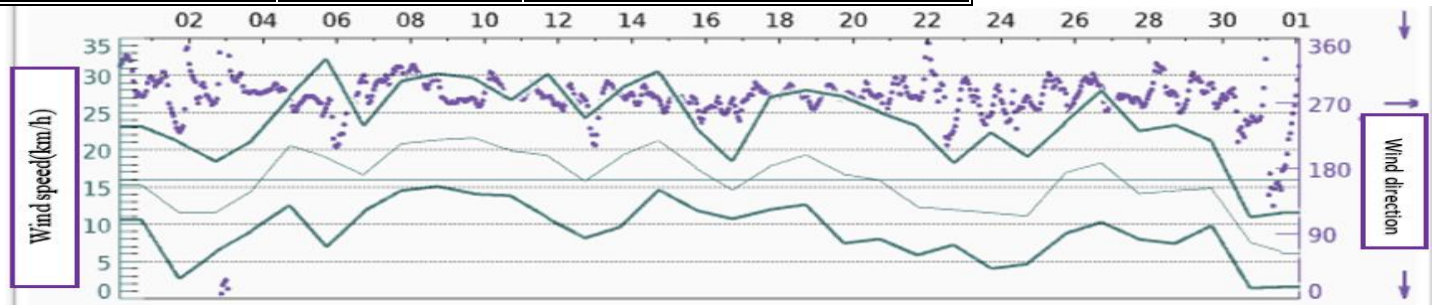

Source No.	S1	S2	S3	S4	S5
Unit Name	flare	Reformer	CR2 (70000)	P.F & CR1 2 3	P1
Source No.	S6	S7	S8	S9	S10
Unit Name	P3	Lub1	Lub2	Lub3 & P2	CR1-70000 & KH

Figure (12) results of the Environmental monitoring and measurement for total emissions from sources.

On-site detection of air pollution sources using mobile devices for a periodic inspection which was conducted for August 2022 for the first air refining unit, which results from the nature of its work in reducing air pollutants and noise levels using hand-held devices, according to the periodic monitoring plan of the Environment Department, and the results were as shown in the **Table (14).**

Table (14) results of the Environmental monitoring and measurement of Air pollution.

Sample date	Sample collection locations	Collection frequency	Measured aspect	Analysis results	Law limits	Comply or Not Comply
1/8/2022	refining unit(1)	3	CO	2	35 ppm for 1 hr	Comply
1/8/2022	refining unit(1)	3	CO_2	336	/	Comply
1/8/2022	refining unit(1)	3	Temp	7 ° C	/	Comply
1/8/2022	refining unit(1)	3	Humdity	64%	/	Comply
1/8/2022	refining unit(1)	3	PM1	0.003	/	Comply
1/8/2022	refining unit(1)	3	PM2.5	0.006	0.025 ppm for 24 hr	Comply
1/8/2022	refining unit(1)	3	PM7	0.032		Comply
1/8/2022	refining unit(1)	3	PM10	0.056	0.1 ppm	Comply

					for 24 hr	
1/8/2022	refining unit(1)	3	TSp	0.087	0.35 ppm for 24 hr	Comply

4.2.2 Examination and Analysis of Water (Before and After Washing the Exchanger)

Laboratory tests and analyzes were divided into two parts: the chemical part (before and after washing) and the biological part the were cultured using sabruod agar media and Nutrient agar.

4.2.2.1 Chemical Part.

a. First: before washing the heat exchanger, Laboratory analyses were carried out on the types of washing water used in the heat exchanger washing process, and accordingly, samples of the water used in the washing process were taken to identify the nature of this water in terms of acidic or basic behaviour, as well as the concentrations of salts (negative and positive ions) in it, and it was found through the examination. As a result, the laboratory showed that this water was within the permissible limits and did not contain any significant concentration of the sulphide ion (S-2), which has a major role in the corrosion process, as shown in the results in **Table 15.**

Table (15) Results of laboratory analyzes of the water used in the washing process in the company (Al-Wasat Refineries - Al Daura Refinery).

Evaluation Criteria	Outcome
Potential of hydrogen	**7.4**
Conductivity of El in µs/cm at 25 C^{O}	**1621**
HCO_3-alkalinity mg/l	**167.75**
$CaCO_3$ hardness mg/l	**384**
$CaCO_3$ Calcium Hardness mg/l	**192**
Hardness as Ca+2 mg/l	**76.8**
$CaCO_3$ Magnesium Hardness mg/l	**192**
Mg+2 hardness mg/l	**46.1**
Chloride mg/l as Cl^-	**216**
Sulphate mg/l as $SO_4^=$	**247.5**
Iron mg/l as Fe	**1.17**
Hydrogen Sulfide mg/l as H_2S	**Nil**
Sodium mg/l as Na	**145**
Potassium mg/l as K	**3.4**

b. **Second: after washing the heat exchanger,** Water after cleaning (heat exchanger) was also analysed in the laboratory, and the results revealed a rise in the amounts of sulphur elements and ions, as well as a drop in the pH function and the release of hydrogen sulphide gas due to its absorption in water. **Tables (16) and (17)** show the results of the wash water analyses after the heat exchanger washing process.

Through the analyses that were conducted for the washing water and the corrosion that occurred in the heat exchanger, the following was observed:

i. The presence of a percentage of chlorine (Cl) in petroleum sediments with traces of calcium (Ca).

ii. Formation of corrosive deposits and scales such as iron sulphide (FeS).

iii. The presence of a percentage of oxygen (O_2) in corrosion areas where oxygen is present in sufficient quantity leads to the formation of iron oxide (FeO), which forms a protective layer at first, but with the presence of an agent to break the protection layer, chlorides or runoff agents lead to the formation of cells with a high concentration of High oxygen content indicates that the cathodic reaction occurs spontaneously, while this possibility decreases with low oxygen content. As for regions with lower oxygen content, they are not effective as cathodes, and the dominant reaction in such a case is the anode interaction, where the behaviour of these regions is like an anode, and then the corrosion that occurs will be the result of oxygen concentration difference cells in terms of the presence of active and negative regions nearby, one of which plays the role of the anode while the other is a cathode.

iv. Oxidation occurs with a small percentage of water in the oil, which leads to pitting on the surface of the metal. The problem is exacerbated by the presence of levels of sulphur, chlorides, and salts to cause a problem of acute pitting erosion caused by concentration difference cells, especially when the layer of iron oxides or iron sulphide, which forms a protective layer at the beginning of corrosion, collapses, leading to severe corrosion. The presence of shear stresses explains the breakdown of this layer. Al Agha et al. [38] and Fontana et al. [39] obtained comparable results.

From the above, it was noted that the amount of oil in the water was high, or in other words, the percentage of oils in the waste water was high throughout the study period. As for the COD examination, it is noted from the results that the results of the examination were good. When comparing the calculations of the results that we have carried out inside the center with the permissible amount of water released to the Iraqi environment, as we can see in the **tables (16 & 17),** We note that most of the results were within the permissible limits, but what concerns us from this study is the percentage of oil, which, as we mentioned earlier, was high.

Table (16) Analysis results after the washing water process.

Evaluation Criteria	Outcome
PH	**6.32**
Electrical conductivity µs /cm at 25 C	**1057**
HCO_3-mg/l alkalinity$^-$	**220**
Magnitude of hardness in mg/l $CaCO_3$	**900**
$CaCO_3$ (mg/l) calcium hardness	**600**
Ca+2 calcium hardness in mg/l	**240**
$CaCO_3$-magnesium hardness mg/l	**300**
Mg +2 mg/l magnesium rigidity	**72**
Cl- (mg/l) chloride	**376**
Sulphate mg/l as $SO_4^=$	**565**
Iron mg/l as Fe	**0.33**
Sulfide % as S^{-2}	**4.8**
H_2S mg/l	**3.4**

Table (17): The laboratory tests of the water used before and after washing the heat exchangers were examined in the laboratory of the Industrial Water Division / Al Daura Refinery.

No	Examination type	Heat exchange wash water	Contaminated water after washing	percentage of environmental determinants
1	PH	7.4	6.32	6-8.5
2	Temp	20.2	27.9	35 C^0
3	SULPHIDE	0.038	4.8	0.5
4	OIL	0.4	67.8	10 ppm
5	COD g/m	0.04	1.39	100 ppm
6	BOD	mg/L 14.1	mg/L 48	40 ppm

7	PHENOL	0.02	0.22	0-0.05 ppm
8	S.S	12	1376	60 ppm
9	CL^-	216	376	100 ppm
10	Turbidity (NTU)	0.81	14.7	
11	PO_4	0.019	0.054	3 ppm
12	SO_4	210	565	+1% of the source 400 ppm
13	DO.	9.8	1.8	
14	T.D.S(ppm)	549	485	Max 1500 ppm

4.2.2.2. Biological Part that were Cultured Using the Following Media

a) Sabruod agar media.
b) Nutrient agar.

After completing the bacteriological implant of the water, no growth of any kind of microorganism was shown for the water samples taken after washing the heat exchanger. This is due to the high percentage of pollution in the water, which acts as an inhibitor to the growth of naturally present microorganisms in natural plants, as shown in **Table 18.** As for the water sample that was taken from the surface of the soil and a sample from a depth of 30 cm only, two types of fungi appeared, namely as shown in **Figure 13 and 14:**

- *Saccharomyces cerevisiae.*

This type of fungus has the ability to grow even in anaerobic conditions and in the absence of oxygen. When present in water, this type provides an amount of CO_2 gas to aquatic plants located beneath the water's surface, i.e., it has the ability to hydrolyze.

- *Penicillium dupontii.*

It is one of the earthy species that exist naturally in normal flora and prefers cold to medium-temperature climates. This type is known for being a lover of organic matter in the soil and for its

high ability to decompose organic matter in the soil (regardless of its source) into simpler and lesser materials. thus, ridding the soil of pollutants.

Reasons for the appearance of fungi without bacteria in the soil:

1. the delay in bacteriological cultivation, and the reason for this is due to the delay in the immediate cultivation process, which led to the death of those living organisms.
2. Because the sample was kept for a long time without being grown in sterile water in glass vials, this made it easier for fungi to grow at the expense of bacteria.
3. The reason for the survival of fungi without bacteria is that fungi, yeasts, and molds are characterized by their ability to survive for a long time, due to the presence of spores. It has, which is a type of reproduction. This stage is characterized by surrounding the germs with a solid outer wall to ensure they are not affected by external conditions. This wall is shattered, and mold begins to grow when the appropriate conditions for growth are available, which are temperature, a nutrient medium, and humidity, as shown in **Figure 13 (A & B).**

Table (18) results of bacteriological implant.

No	Model name	The medium used	Results
1	A sample of water taken from the surface of the soil and a sample from a depth of 30 cm	Sabrod agar, Nutrient agar	*Pencillum, Saccharomyces cervisiae*
2	Sample water after washing the heat exchanger	Sabrod agar, Nutrient agar	No growth

Figure(13) (A)Form of yeast (*Saccharomyces cervisiae*) in Agricultural medium &(B) fungus (*pencellium*).

Figure (14) (A)surface of the soil and (B) a sample from a depth of 30 cm.

4.2.3 Soil Contamination with (Fouling)

4.2.3.1 Chemical Part

Other chemical tests were conducted on soil samples brought from different locations of the Central Refineries Company, where some samples were taken and soil measurement methods were applied to them, including cations and anions present in the soil with hydrocarbons mixed with the soil. It was found from the laboratory examination that all samples taken contain a high percentage

of hydrocarbons, as shown in **Figure 15 (A-E).** The laboratory work included conducting direct examinations, as shown in **Table 19.**

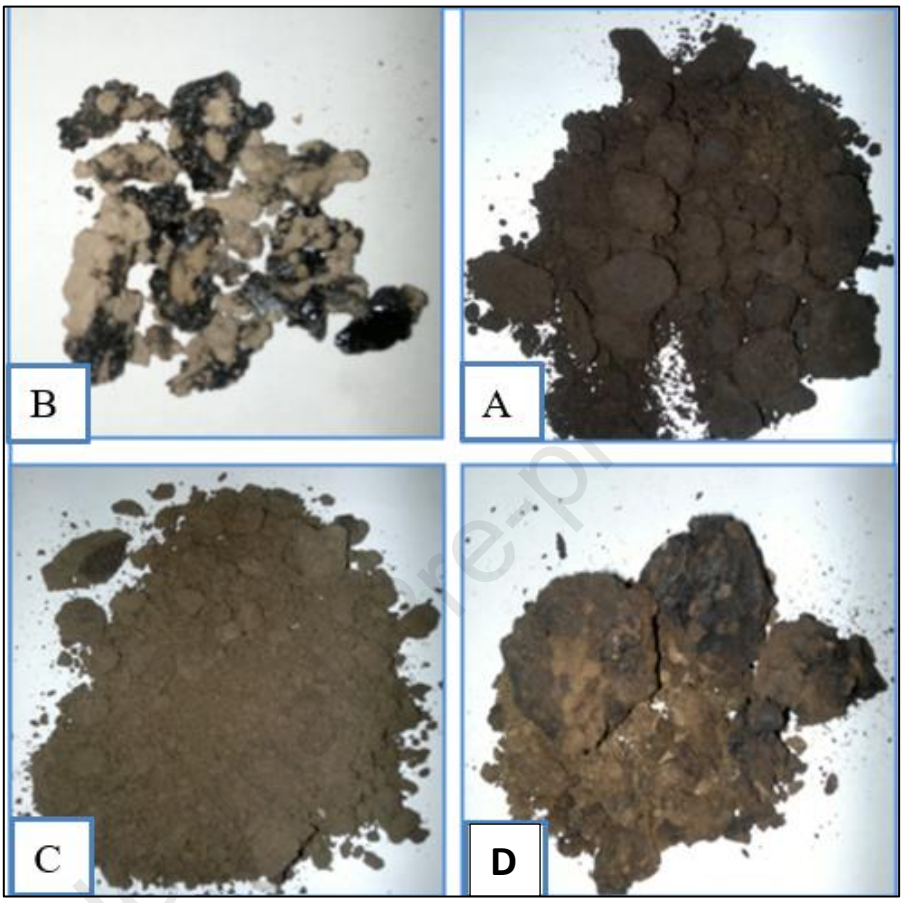

Figure (15) (A) a soil sample from the heat exchanger washing site, (B) a soil sample surrounding the construction site of the refining unit (E10- Czech), (C) a soil sample surrounding the crude oil depot, (D) a random soil sample from the refinery AL-Daura (Baghdad -AL-Iraq).

Table (19) the results of chemical analyzes of the soil.

TEST	Form No (1)	Form N(2)	Form N(3)
PH	6.95	7.2	7.2
Total hardness mg/l as $CaCO_3$	552	436	421

Ca^{+2}	mg/l	126	105.92	114.25
Mg^{+2}	mg/l	57	41.1	32.49
Fe	mg/l	2.9	10.4	8.8
Cd	mg/l	1.2	1.05	2.2
Pb	mg/l	3.2	1.66	4.6
Cu	mg/l	6.6	4.33	8.65
SO_4^{-2}	mg/l	58.6	72.3	52.4
Cl^{-1}	mg/l	22.36	16.86	15.54
Hydro carbon %		Very, very high percentage	Very, very high percentage	Very, very high percentage

4.2.3.2 Biological Part Implant Using the Following Media

One gram of contaminated soil was taken, added to 30 ml of distilled water, and kept in tightly closed glass containers containing boiled and cooled distilled water inside. Its purpose is to create a sterile medium for the growth of microorganisms and to prevent contamination with any other organisms from the surrounding atmosphere. Note that this step was carried out inside the site, after which the samples were brought to the laboratory and planted in the following media:

a. **Macconkey Agar**

This type of media is special for "gram stain" negative bacteria, and its purpose is to facilitate the process of isolating this type of bacteria. The culture conditions for this medium were at a temperature of (42 degrees Celsius and in aerobic conditions, meaning oxygen must be available here.

b. Nutrient Agar

This type of medium is a general medium that helps the growth of all kinds of microorganisms. The culture was carried out under aerobic conditions. It is meant here as a medium that contains several types of nutrients, as this medium contains (10%) sterilized blood, Peyton, sodium chloride, cow extract (beef extract), and yeast extract, and one of the conditions that must be available in this medium is that the pH ranges from (7-7.6) and the temperature is 42 degrees Celsius).

c. **Subrod Agar:**

This type of media is an optional medium for fungus and mold, and it consists of tryptone and peptone, as well as a pH of 5.6.

These media were prepared by taking a certain weight of the soil and dissolving it in a certain volume of distilled water, and then the sterilization process is done through the (autoclave) device, after which it is poured into special clean and sterilized agricultural dishes used for this purpose and left for a period until it solidifies, after which the model is taken by means of a special tool (the loop). The bacteriological diagnosis was carried out in Al-Mustansiriya University's soil laboratory in the College of Science and Life Sciences., and the results are shown in **Table 20** below.

Table (20) shows the results of bacteriological implant.

Sample	Macconky agar	nutrient agar	Notes
1	Small reddish-pink colonies appear	Appearance of translucent pale colonies	*Streptococcus* bacteria
2	The appearance of pink colonies	The appearance of pale-coloured colonies	*Streptococcus* bacteria
3	Very small pink colonies appear	The appearance of pale, medium-sized colonies	*E. coli* bacteria
4	Large pink colonies appear	No mold growth was seen on the medium	lost isolation due to the rising temperatures

- Fungi grown on Subrod agar medium did not grow, except in model No. 1, where a *Pencillum* type fungus grew near the heavy sewage pipes.

Through the diagnosis of the results of bacteriological culture, it was found that two types of bacteria and a type of fungus appeared in the soil taken, which are:

- *E. coli* and *Streptococcus*, both bacteria.
- *Penicillium* is a type of fungus.

where both the first and the second are known to be widespread bacteria. The third is known as a type of fungus that is widespread in the environment in general. Each type of living organism

has an accurate scientific classification that is known and proven globally, according to the classification of each genus of these organisms.

As for the mold that appeared, it is of the type *Penicillium dupontii*, and each fungus has its own global classification (genus), and it is one of the earthy species found naturally (normal flora). It loves the organic materials present in soil and has the ability to analyse the organic materials into simpler and less complex materials.

i. All the soils taken are polluted with a very high percentage of hydrocarbons.
ii. The sample of polluted soil taken from the heat exchanger wash site was thick and solid.
iii. The laboratory results of the rest of the ions present in the polluted soil were not balanced due to the high percentage of hydrocarbon compounds polluting the soil.

4.2.4 X-Ray Fluorescence (XRF)

The analyses were performed on soil sediment samples, and the results of the preliminary statistical analysis of the data are shown in **Tables (21&22).** Limits of XRF detection and quantification of most elements were appropriate. Generally, a soil sample was taken from the heat exchanger washing sites for elemental analysis, and heavy metal concentrations were calculated using XRF. The result showed the concentrations of elements in the soil in the range of copper (0.952%), zinc (0.725%), sodium (0.677%), potassium (0.439%), chlorine (0.432%), phosphorus (0.162%), Ti (0.2%), and chromium (0.138%). Apart from Ni, As, Sr, Mo, Ba, V, and a, the remaining concentrations in this pool showed relatively low concentrations but were still around their final values. 1-4%. The highest concentrations were found only in Ca (30.015), Fe (15.507), Si (6.081), S (5.712), Mg (2.279), and Al (1.780). Soil contamination with heavy metals at the Al Daura refinery and its environs is high. A similar result was obtained by Ogundare., [40], Kadem et al. [41], and Oguntimehin etal.,[42].

Table (21) XRF for Elemental Concentrations (soil).

Name	Z (Atomic number)	Value
Na	11	0.677
Mg	12	2.279
Al	13	1.780
Si	14	6.081
P	15	0.162
S	16	5.712

Cl	17	0.432
K	19	0.439
Ca	20	30.015
Ti	22	0.200
V	23	0.026
Cr	24	0.138
Mn	25	0.105
Fe	26	15.507
Ni	28	0.085
Cu	29	0.952
Zn	30	0.725
As	33	0.011
Sr	38	0.499
Mo	42	0.012
Ba	56	0.070

Table (22) XRF for elemental (soil).

Name	Z (Atomic number)	Value
Na_2O	11	0.958
MgO	12	3.980
Al_2O_3	13	3.185
SiO_2	14	12.327
P_2O_5	15	0.306
SO_3	16	11.661
Cl	17	0.356
K_2O	19	0.441
CaO	20	34.193
TiO2	22	0.247
Cr_2O_3	24	0.164
MnO	25	0.102
Fe_2O_3	26	16.396
NiO	28	0.086
CuO	29	0.932
ZnO	30	0.655
SrO	38	0.655
Zro_2	40	0.420
MoO_3	42	0.014

4.2.5 X-Ray Diffraction (XRD)

X-ray diffraction studies were conducted on soil contaminated with (fouling) to discover new mineral formations that could critically influence the strength of soil behavior. **Figure 16** presents the results of the scanning electron microscopy test using EDAX. The results showed that 1.4% is composed of copper metal, and the lack of copper in the polluted soil is due to the high pH and soil pressure. The higher percentage is due to carbon at 455%) This increase is expected because carbon is an organic substance, and the basis for this increase is soil pollution (fouling). These deposits are formed due to heating the crude oil inside the heat exchanger. The effect of oil pollution on some geotechnical properties was clearly observed in soils subjected to fouling. Furthermore, because fouling behaves similarly to water, it increases the possibility of slipping between particles, lowering the shear strength of fouling soil. A similar result was obtained by Zamani et al. [43].

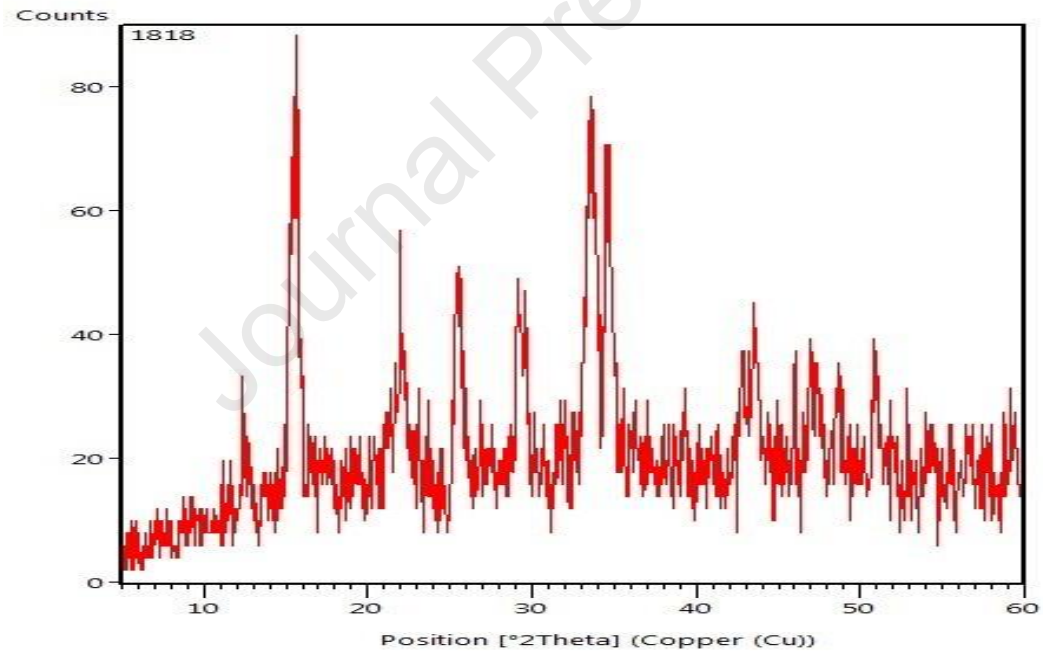

Figure (16) XRD results for the untreated contaminated soil sample.

4.2.6 Scanning Electron Microscope (SEM-EDS) Analysis

SEM analysis is used to characterize the obtained structural and microscopic images shown in **Figure 17** at magnifications of about 5 µm, 1 µm, and 0–20 nm, respectively. In these figures, it was observed that nanoparticles and glass fibres had an average particle size of about 100 nm, a uniform surface area, and a spherical shape. However, since SEM analysis was used to determine particle size, the results were unreliable and insufficient to establish statistical results for particle size distribution because it is measured in tens to hundreds among many particles. This is confirmed by the results of Devendiran et al. [44].

Table 23 presents that the amount of magnesium and aluminum in polluted soil is lower than that of silicon in the iron and copper content in contaminated soils is higher than in uncontaminated soils, and an increase in sulphur content is observed. The geological characteristics, climatic characteristics, and mechanical performance of stable polluted soils are all influenced by changes in the nanoscale formation of these soils. SEM image of the unprocessed, tainted material is depicted in **Figure 17.** The image reveals clinker grains composed of silt, clay fragments, and a trace of fine sand as a framework between the grains, with the clay particles arranged in inherently unstable patterns that give rise to visible gaps and the crumbling of the fine grains. The XRD study demonstrated that the clay particles present in the distributed mixture contained Figure 17 (A to J) and integrated free minerals (calcium, silica, iron, sulphur, magnesium, aluminium, etc.) into its substructure. These results corroborated the study's findings [46-48].

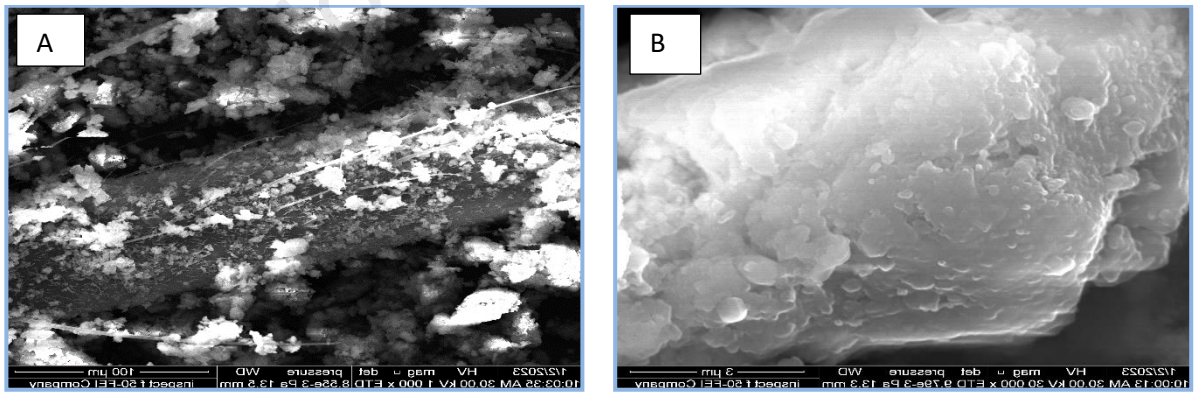

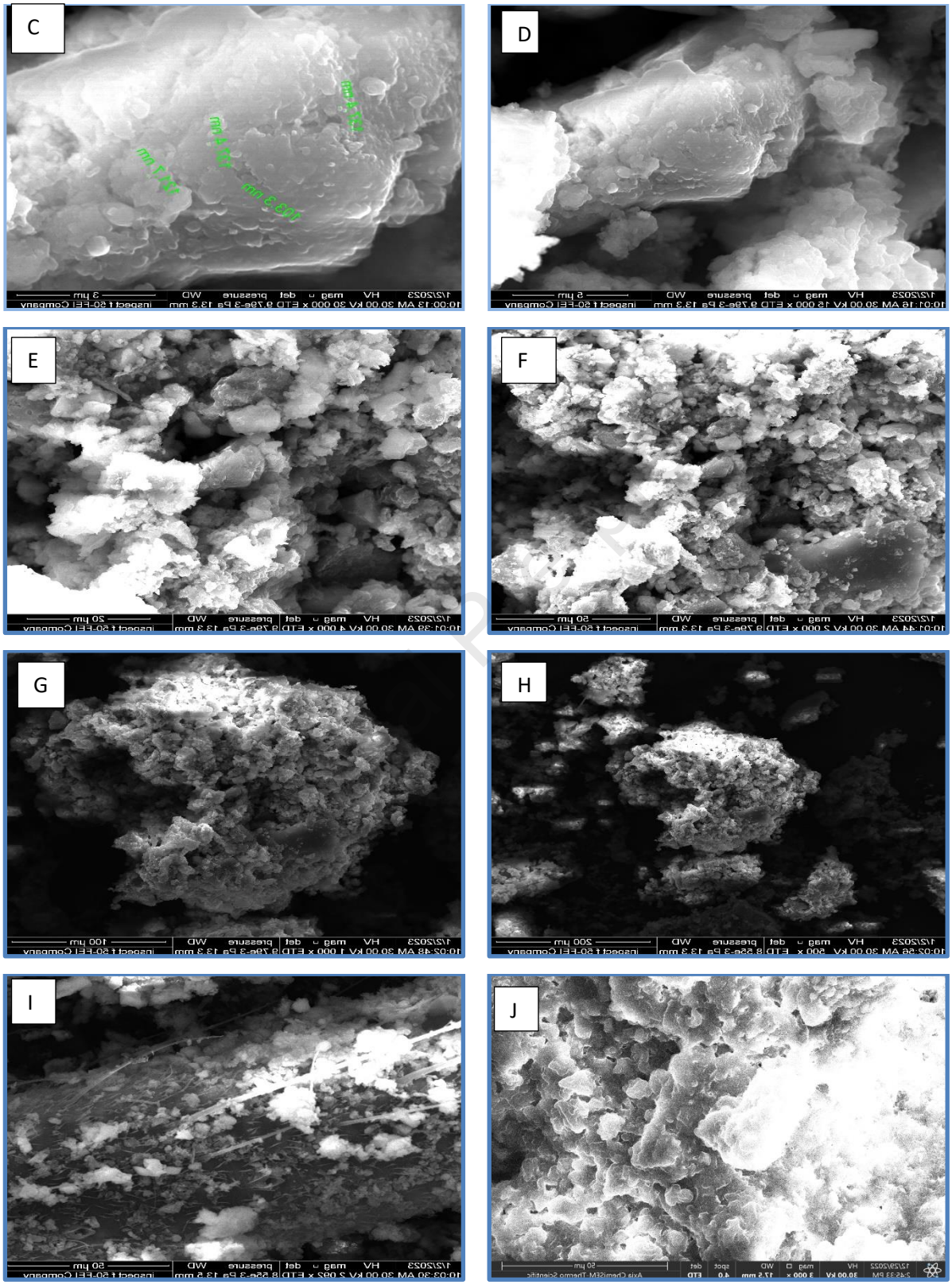

Figure (17) SEM -EDS images of contaminated soil.

This work also analyzed elements on the top of earth granules using energy-dispersive X-ray spectroscopy (EDS). The proportional chemical changes caused by the impacts of pollutants were observed by recording the highest strength at various periods. The clean polluted sample in **Table (23)** and **Figure (18)** had Ca (Figure 18 H), Si (Figure 18 F), O (Figure 18 B), Al (Figure 18 E), Mg (Figure 18 D), Cu (Figure 18 I), and Fe (Figure 18 C), S as its key elements ((Figure 18 G). In addition, all of the cured samples showed high-intensity peaks for both silicon (c) and oxygen (o), though to varying degrees. This is consistent with the finding [42]**.** No lead or cadmium was found, as evidenced by the soil's hardened structure.

Table (23) EDS for elemental distribution in contaminated soil.

Element	Atomic %	Atomic % Error	Weight %	Weight % Error
C	64.5	0.6	45.5	0.4
O	20.4	0.4	19.2	0.4
Mg	0.8	0.1	1.1	0.1
Al	0.9	0.0	1.4	0.1
Si	2.2	0.0	3.6	0.1
S	2.5	0.0	4.7	0.1
Ca	4.7	0.1	11.2	0.1
Fe	3.6	0.1	11.9	0.2
Cu	0.4	0.0	1.4	0.2

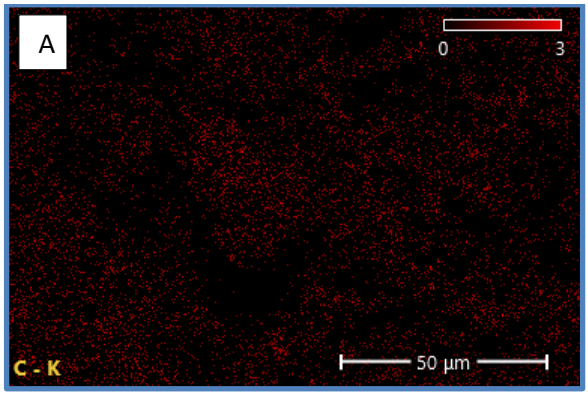

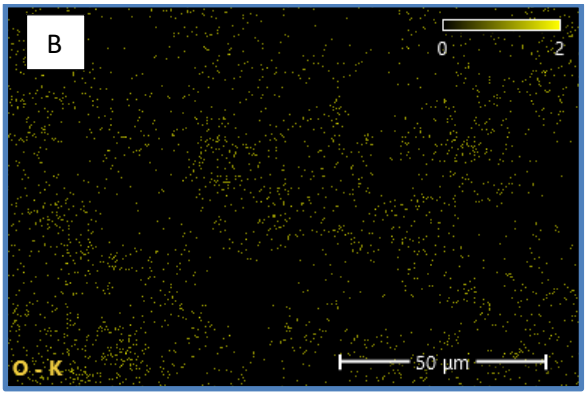

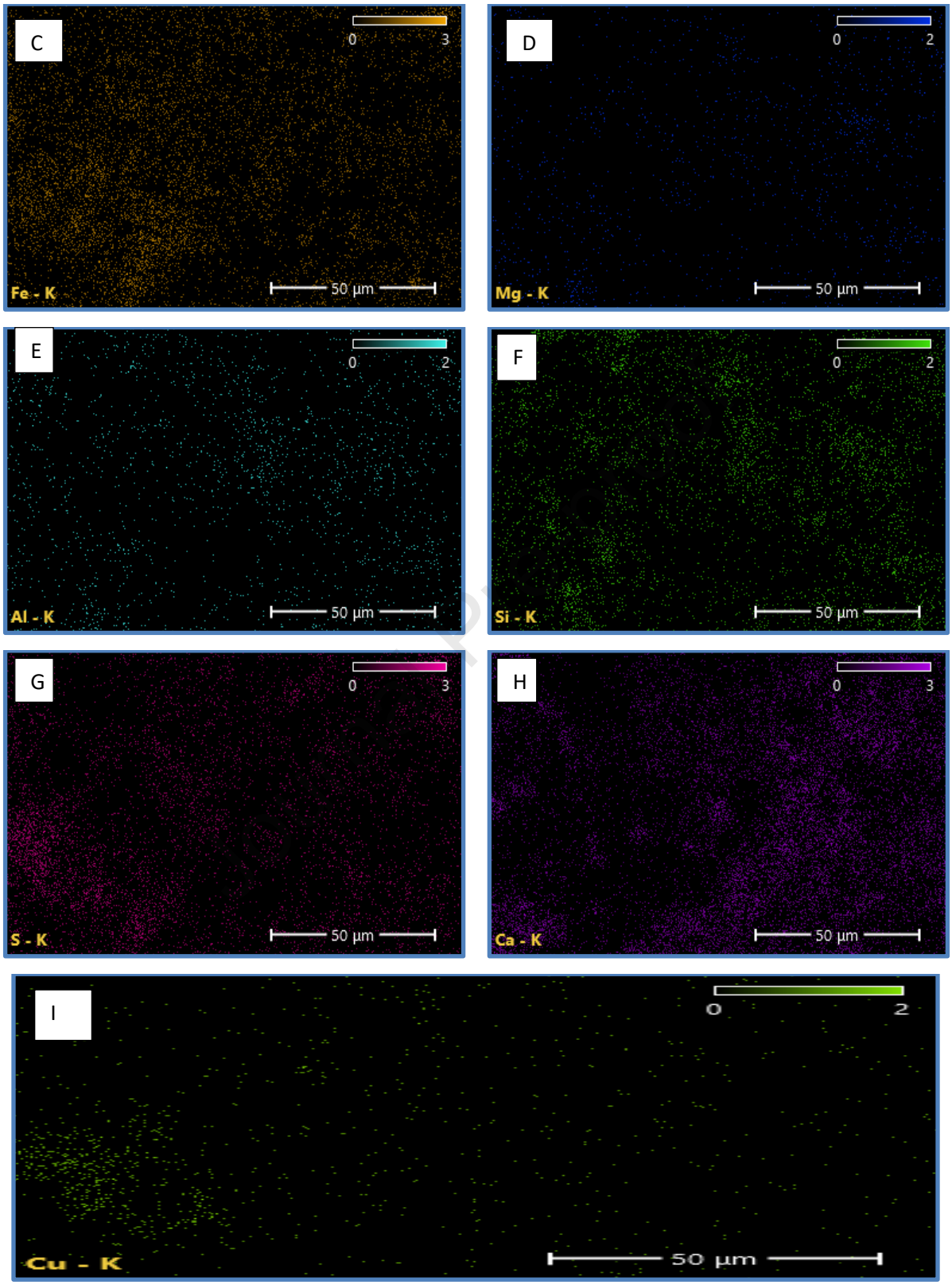

Figure (18) SEM-EDS Shows the distribution of element spaces in the soil; **A)** C, **B)** O, **C)** Fe, **D)** Mg, **E)** Al, **F)** Si, **G)** S, **H)** Ca, **I)** Cu.

5. Conclusions

The fouling coefficient and the decrease in the heat exchange product identified the most essential factors inherent in nutrition and causing fouling. It was found that fouling leds to a reduction in thermal productivity by 7.3%. In addition, it was concluded that it is possible to know the nature and shape of the sediment, the particle size, and the percentage of elements that enter into the formation of fouling and its oxides, using various devices such as XRD, XRF, and SEM-EDS

It was found that the area with the most pollution outside of the refinery was near the highway next to the refinery. This was because it was on the pollution spread line and the direction of the wind was usually from this direction.

Moreover, the amount of energy required to refine a cubic meter of refined crude oil was calculated during august and is equal to **165** Megajoules / cubic meter, compared to the average standard value of energy required to refine a cubic meter of crude oil, which was calculated in the range of 2299 megajoules / cubic meter. The difference in energy consumed for August was 7%, which reduces the burden on the environment and the amount of fuel consumed.

The average energy consumption of the Daura Refinery Company was calculated, and its value was **2299** megajoules / cubic meter, as the best two years of energy values recorded for the years 2016–2019 were approved and considered a standard value for comparison.

Through the diagnosis of the results of bacteriological culture, it was found that two types of bacteria and a type of fungus appeared in the soil taken, which are *E. coli, Streptococcus* and *Penicillium* is a type of fungus. Reasons for the emergence of fungi without bacteria in the soil include: First: There was a delay in bacteriological culture, and the reason for this was the delay in the process of immediate cultivation, which led to the death of those organisms. Second: The long period during which the sample was left preserved without cultivation in glass bottles containing sterile water helped the growth of fungi at the expense of bacteria. Third: The reason for the survival of fungi without bacteria is that fungi, yeasts, and molds are characterized by their ability to survive. This stage is characterized by surrounding the spore with a hard outer wall to ensure that it is not affected by external conditions. This wall is shattered, and mold begins to grow when the appropriate temperature, nutrient medium, and humidity conditions are available for growth. Moreover**,** it was found that all of the samples had a high percentage of hydrocarbons. and The soil model surrounding the site of washing the heat exchangers was oil itself mixed with a small percentage of the soil, and the optimal treatment for this kind of soil pollution is the process

of scraping the soil and thus burying the material that was scraped, and then breaking up this soil through plowing and exposing it to the atmosphere.

It has been found that the water contaminated with fouling after completing the bacteriological implant of the water, no growth of any kind of microorganism was shown for the water samples taken after washing the heat exchanger. This is due to the high percentage of pollution in the water, which acts as an inhibitor to the growth of naturally present microorganisms in natural plants. In addition, the presence of a certain amount of chlorine (Cl) in petroleum sediments that also have small amounts of calcium (Ca). The Formation of corrosive deposits and scales such as iron sulphide (FeS).Moreover, the presence of a percentage of oxygen (O_2) in corrosion areas where oxygen is present in sufficient quantity leads to the formation of iron oxide (FeO), which forms a protective layer at first, but with the presence of an agent to break the protection layer, chlorides or runoff agents lead to the formation of cells with a high concentration of High oxygen content indicates that the cathodic reaction occurs spontaneously, while this possibility decreases with low oxygen content. As for regions with lower oxygen content, they are not effective as cathodes, and the dominant reaction in such a case is the anode interaction. The behaviour of these regions is like an anode, and then the corrosion that occurs will result from oxygen concentration difference cells in terms of the presence of active and negative regions nearby, one of which plays the role of the anode while the other is a cathode. Even more, oxidation occurs with a small percentage of water in the oil, which leads to pitting on the surface of the metal. The problem is exacerbated by the presence of levels of sulphur, chlorides, and salts to cause a problem of acute pitting erosion caused by concentration difference cells, especially when the layer of iron oxides or iron sulphide, which forms a protective layer at the beginning of corrosion, collapses, leading to severe corrosion. The presence of shear stresses explains the breakdown of this layer. Hence, it is highly recommended to development of insulators or gizzards for H_2S, and investigate the possibility to reduce the percentage of sulphur oxides by making maximum use of the available heat by ensuring complete combustion of the fuel and increasing the temperature and pressure of the steam produced, in addition to testing the ideal ratio of fuel and air and finally performing periodic maintenance on the boiler parts.

Limitations of the Study

The main limitation of this study is the restricted availability of actual samples directly from the refinery process. Obtaining these samples is a challenging and infrequent task, as it can only be accomplished during the rare biannual shutdowns in the refinery system.

Acknowledgments

The authors would like to thank Mustansiriyah University (www.uomustansiriyah.edu.iq) Baghdad-Iraq for their support in the current work. The authors also would like to acknowledge the support of University of Birmingham UK for their valuable support and acknowledge the support of AL Daura Refinery and Oil Research and Development Center, Baghdad, Iraq.

Author contributions

Z.T., propose the work and M.A designed the experiments. Z. A, conduct the experimetal work in collaboration with Z.T. M.A H.O wrote the paper. Z.T, Z.A: Performed the experiments. Z.A, Z.T., M.A Analyzed and interpreted the data..

Conflict of interest

The authors confirm that there is no conflict of interest.

Data Availability

Data will be made available on request

References

1. J. Taborek, T. Aoki, R.B. Ritter, J.W. Palen, J.G. Kundsen. Predictive Methods for Fouling Behavior. Chem Eng Prog. 1972;68(7):69-7.
2. B.L. Yeap. Designing Heat Exchanger Networks to Mitigate Fouling [PhD Thesis]. Cambridge (UK): Cambridge University; 2003.
3. J.H. Lavaja, M.J. Bagajewicz. On a New MILP Model for the Planning of Heat-Exchanger Network Cleaning. Industrial & Engineering Chemistry Research. 2004;43(14):3924–3938.
4. D.I. Wilson, G.T. Polley, S.J. Pugh. Mitigation of crude oil preheat train fouling by design. Heat Transfer Eng. 2002;23(1):24-37.
5. ESDU. Heat exchanger fouling in the pre-heat train of a crude oil distillation unit, Data Item 00016. London, ESDU International plc, 2000.
6. F. Coletti, S. Macchietto. Refinery pre-heat train network simulation undergoing fouling: assessment of energy efficiency and carbon emissions. Heat Transfer Eng. 2011;32(3-4):228-236.

7. F. Coletti, S. Macchietto. Minimising efficiency losses in oil refineries: a heat exchanger fouling model. In: Sustainable Energy UK: Meeting the science and engineering challenge. St Anne's College, Oxford; 2008.
8. C.B. Panchal, W.C. Kuru, C.F. Liao, W.A. Ebert, J.W. Palen. Threshold conditions for crude oil fouling. In: Understanding Heat Exchanger Fouling and Its Mitigation. Castelvecchio Pascoli, Italy: Begell House Inc; 1999.
9. J.G. Speight. Chemical Process and Design Handbook. 1st ed. New York: McGRAW-HILL; 2002. [Accessed from https://www.accessengineeringlibrary.com/content/book/9780071374330]
10. Z. Abdulhussein, Z. Al-sharify, M. Alzuraiji, H. Onyeaka. Environmental Significance of Fouling on the Crude Oil Flow. A Comprehensive Review: Fouling on The Crude Oil Flow. Journal of Engineering and Sustainable Development. 2023 May 1;27(3):317-38.
11. O.E. Essien, I.A. John. Impact of crude-oil spillage pollution and chemical remediation on agricultural soil properties and crop growth. Journal of Applied Sciences and Environmental Management. 2010;14(4). https://doi.org/10.4314/jasem.v14i4.63304.
12. A.Samimi, A. Bagheri, S. Dokhani, S. Azizkhani, E. Godini. Solution for Corrosion Reducing Gas Pipe Line with Inspection for Preventing Fouling in Oil Exchangers. International Journal of Basic & Applied Sciences. 2013;2(2). Available at https://www.researchgate.net/publication/274719128_Solution_for_Corrosion_Reducing_Gas_Pipe_Line_with_Inspection_for_Preventing_Fouling_in_Oil_Exchangers.
13. J.K. Pental. Design and commissioning of a crude oil fouling facility. Doctoral dissertation, Imperial College London. 2012.
14. H. Guo, Y. Sun, X. Wang. Spatial Distribution Characteristics and Source Analysis of Heavy Metals in County Urban Soil. Journal of Environmental Science. 2022;42:287-297.
15. I.L. Pepper, C.P. Gerba, T.J. Gentry, R.M. Maier (Eds.). Environmental microbiology. Academic press. 2011.
16. A.N. Al-Ghadhban, N. Al-Majid. Oil Pollution. Regional Organization for the Protection of the Marine Environment; 2009.
17. American Petroleum Institute. Corrosion of Oil-and Gas-well Equipment. Corrosion Engineering. American Petroleum Institute PETRO-LTD; 1990.
18. H. Müller-Steinhagen, M.R. Malayeri, A.P. Watkinson. Heat Exchanger Fouling: Environmental Impacts. Heat Transfer Engineering. 2009;30(10-11):773–776.
19. A.M. Hadi, A.K. Mohammed, H.J. Jumaah, M.H. Ameen, B. Kalantar, H.M. Rizeei, Z.T.A. Al-Sharify. GIS-Based Rainfall Analysis using Remotely Sensed Data in Kirkuk Province, Iraq: Rainfall Analysis. Tikrit Journal of Engineering Sciences. 2022;29(4):48–55. https://orcid.org/0000-0002-5786-8236.
20. H. Zaid, Z. Al-sharify, M.H. Hamzah, S. Rushdi. Optimization Of Different Chemical Processes Using Response Surface Methodology - A Review: Response Surface Methodology. Journal of Engineering and Sustainable Development. 2022;26(6):1-12. https://doi.org/10.31272/jeasd.26.6.1.
21. N.Q. Hussein, S.S. Muhsun, Z.T. Al-Sharify, H.T. Hamed. Experimental And CFD-Simulation of Pollutant Transport in Porous Media. Journal of Engineering and Sustainable Development (JEASD). 2021;25(4). https://doi.org/10.31272/jeasd.25.4.3.
22. A.H. Khalaf, M.S. Rajab. Crude Oil Desalting Using Multi-Surfactant Based on a Best Dosage, Solvent and Mixing Ratio. Tikrit Journal of Engineering Sciences. 2019;26(2):23–27. https://doi.org/10.25130/tjes.26.2.04.

23. F.M. Muhauwiss, S.S. Hassoun. Wetting and Drying Cycles Effect on Durability of Gypsum Soils Treated With Calcium Chloride Or Cement Additives. Tikrit Journal of Engineering Sciences. 2021;28(2):80–92.
24. S.J. Pugh, G.F. Hewitt, H. Müller-Steinhagen. Heat Exchanger Fouling in the Pre-Heat Train of a Crude Oil Distillation Unit-The Development of a User Guide. "Heat Exchanger Fouling-Fundamental Approaches and Technical Solutions." 2002;201-212.
25. M. Parfi. Future Power. National Geographic. 2005;208(2):2–31.
26. ESDU Report. Heat Exchanger Fouling in the Pre-Train of Crude Oil Distillation Unit. ESDU International, London, UK; 2007.
27. H. Müller-Steinhagen, M.R. Malayeri, A.P. Watkinson. Recent Advances in Heat Exchanger Fouling Research. Heat Transfer Engineering. 2007;28(3):173–176.
28. F.S. Liporace, S.G. De Oliveira. Real Time Fouling Diagnosis and Heat Exchanger Performance. Heat Transfer Engineering. 2007;28(3):193–201.
29. T. Graupner, A. Kassahun, D. Rammlmair, J.A. Meima, D. Kock, M. Furche, et al. Formation of sequences of cemented layers and hardpans within sulfide-bearing mine tailings (Mine District Freiberg, Germany). Appl. Geochem. 2007; 22:2486–2508. doi:10.1016/j.apgeochem.2007
30. W. Wei, F. Sun, Y. Shi, L. Ma. Theoretical prediction of acid dew point and safe operating temperature of heat exchangers for coal-fired power plants. Appl. Therm. Eng. 2017;123:782–790.
31. J. Abeywickrama, M. Grimmer, N. Hoth, T. Grab, C. Drebenstedt. Geochemical characterization of fouling on mine water driven plate heat exchangers in Saxon mining region, Germany. Int J Heat Mass Transfer. 2021;176:121486.
32. Helalizadeh et al. Chemical Engineering Science. 2006;61:2069–2078. https://www.elsevier.com/books/environmental-and-pollution-science/pepper/978-0-08-049479-1.
33. J. Chew, H.M. Joshi, S.G. Kazarian, M. Millan-Agorio, F.H. Tay, S. Venditti. Deposit characterization and measurements. In: F. Coletti, G.F. Hewitt, editors. Crude oil fouling. First Elsevier Inc; p. 95–178. http://dx.doi.org/10.1016/B978-0-12-801256-7.00004-X; 2015.
34. G. Brons, L.D. Brown, H.M. Joshi, R.J. Kennedy, T. Bruno, T.M. Rudy. Method for refinery foulant deposit characterization. US 2006/0014296Al; 2006.
35. S. Venditti, C. Berrueco, P. Alvarez, T.J. Morgan, M. Millan, A.A. Herod, et al. Developing characterization methods for foulants deposited in refinery heat exchangers. In International Conference on Heat Exchanger Fouling and Cleaning, Volume VIII. Schladming, Austria; 2009. p. 44–51.
36. W. Greif, K. Klemm. Influence of arsenic from anthropogenic loaded soils on the mine water quality in the tin district Ehrenfriedersdorf, Erzgebirge (Germany). Eng Life Sci. 2008;8:631–640. doi: 10.1002/elsc.200800034.
37. N. Epstein. Thinking about heat transfer fouling: a 5_5 matrix. Heat Transf Eng. 1983;4(1):43–56.
38. O. Al Agha. "Corrosion in structures." J. Al-Aqsa University. 2006;10(S.E.).
39. M.G Fontana, R.W. Staehle. "Advances in Corrosion Science & Technology." Plenum Press-New York and London, Vol. 5. 1976.
40. O.F. Ogundare. Heavy Metal Pollution by Human Activities of Selected Centers within Akure. M. Tech. Thesis. The Federal University of Technology, Akure, Nigeria. 1998.

41. D.E. D. Kadem, O. Rached, A. Krika, Z. Gheribi-Aoulmi. Statistical analysis of vegetation incidence on contamination of soil by heavy metals (Pb, Ni and Zn) in the vicinity of an iron steel industrial plant in Algeria. Environmetrics. 2004;15:447–462.
42. I. Oguntimehin, K. Ipinmoroti. Profile of heavy metal from automobile workshops in Akure, Nigeria. Environ. Sci. and Tech. 2008;1(1):19–26.
43. M.M. Zamani, M. Fallahpour, G.Y. Harvani, S.K. Aghmiuni, M. Zamani, D.M. Tehrani, G.S. Firrozabadi. Recent proportionate treatment methods for crude oil contamination evaluation of the Tehran refinery site soil. Thrita. 2014;3(1).
44. D.K. Devendiran, V.A. Amirtham. A review on preparation, characterization, properties and applications of nanofluids. Renewable Sustainable Energy Rev. 2016;60:21-40.
45. H.J. Kadhim, K.A. Saeed, N.O. Kariem. Using geopolymers materials for remediation of lead-contaminated soil. Pollut Res. 2019;38(4):85–95.
46. Z.T. Al-Sharify, M. F. Lahieb, L.B. Hamad, H.A Jabbar. A review of hydrate formation in oil and gas transition pipes (2020) IOP Conference Series: Materials Science and Engineering, 870 (1), art. no. 012039. https://doi.10.1088/1757-899X/870/1/012039
47. K.A. Saeed, S.A. Hashim. The morphology and elemental variation for contaminated clay soil using Energy Dispersive X-Ray Spectrometry 2020. In IOP Conference Series: Materials Science and Engineering. 2020;737(1):012082.

You Declaration of interests

☒ The authors declare that they have no known competing financial interests or personal relationships that could have appeared to influence the work reported in this paper.

☐The authors declare the following financial interests/personal relationships which may be considered as potential competing interests: